



JGR Biogeosciences

RESEARCH ARTICLE

10.1029/2021JG006276

Special Section:

Understanding carbon-climate feedbacks

Key Points:

- An unmanaged evergreen forest has been a net carbon sink for over 25 years and the sink strength has increased significantly with time
- Annual average carbon increment measured by eddy flux or inventory data are not significantly different
- The forest remained a robust C sink in the warmest, wettest, and driest years since 1895, indicating resistance to climate variability

Supporting Information:

Supporting Information may be found in the online version of this article.

Correspondence to:

D. Y. Hollinger, david.hollinger@usda.gov

Citation

Hollinger, D. Y., Davidson, E. A., Fraver, S., Hughes, H., Lee, J. T., Richardson, A. D., et al. (2021). Multi-decadal carbon cycle measurements indicate resistance to external drivers of change at the Howland Forest AmeriFlux site. *Journal of Geophysical Research: Biogeosciences*, 126, e2021JG006276. https://doi.org/10.1029/2021JG006276

Received 22 FEB 2021 Accepted 15 JUN 2021

Author Contributions:

Conceptualization: D. Y. Hollinger, E. A. Davidson, S. Fraver, A. D. Richardson, K. Savage, D. Sihi, A. Teets Data curation: D. Y. Hollinger, E. A. Davidson, H. Hughes, J. T. Lee, A. D. Richardson, K. Savage, D. Sihi, A. Teets Formal analysis: D. Y. Hollinger, E. A. Davidson, S. Fraver, A. D. Richardson, K. Savage, D. Sihi, A. Teets

© 2021. American Geophysical Union. All Rights Reserved. This article has been contributed to by US Government employees and their work is in the public domain in the USA.

Multi-Decadal Carbon Cycle Measurements Indicate Resistance to External Drivers of Change at the Howland Forest AmeriFlux Site

D. Y. Hollinger¹, E. A. Davidson², S. Fraver³, H. Hughes³, J. T. Lee³, A. D. Richardson^{4,7}, K. Savage⁵, D. Sihi⁶, and A. Teets⁷

¹USDA Forest Service, Northern Research Station, Durham, NH, USA, ²Appalachian Laboratory, University of Maryland Center for Environmental Science, Cambridge, MD, USA, ³School of Forest Resources, University of Maine, Orono, ME, USA, ⁴School of Informatics, Computing, and Cyber Systems, Northern Arizona University, Flagstaff, AZ, USA, ⁵Woodwell Climate Research Center, Falmouth, MA, USA, ⁶Department of Environmental Sciences, Emory University, Atlanta, GA, USA, ⁷Center for Ecosystem Science and Society, Northern Arizona University, Flagstaff, AZ, USA

Abstract A long-standing goal of ecology has been to understand the cycling of carbon in forests. This has taken on new urgency with the need to address a rapidly changing climate. Forests serve as long-term stores for atmospheric CO_2 , but their continued ability to take up new carbon is dependent on future changes in climate and other factors such as age. We have been measuring many aspects of carbon cycling at an unmanaged evergreen forest in central Maine, USA, for over 25 years. Here we use these data to address questions about the magnitude and control of carbon fluxes and quantify flows and uncertainties between the different pools. A key issue was to assess whether recent climate change and an aging tree population were reducing annual C storage. Total ecosystem C stocks determined from inventory and quantitative soil pits were about 23,300 g C m⁻² with 46% in live trees, and 48% in the soil. Annual biomass increment in trees at Howland Forest averaged 161 ± 23 g C m⁻² yr⁻¹, not significantly different from annual net ecosystem production (NEP = -NEE) of 211 ± 40 g C m⁻² y⁻¹ measured by eddy covariance. Unexpectedly, there was a small but significant trend of increasing C uptake through time in the eddy flux data. This was despite the period of record including some of the most climate-extreme years in the last 125. We find a surprising lack of influence of climate variability on annual carbon storage in this mature forest.

Plain Language Summary Trees remove carbon dioxide (CO₂) from the atmosphere by photosynthesis and store it in chemical form in wood and other plant tissues. Much of the stored carbon ends up in the soil. Plants and soil organisms use some of the stored carbon to provide energy for growth and plant maintenance processes which releases CO₂ back to the atmosphere. The movement of carbon atoms into and out of the forest and through the plants and soils is termed the "carbon cycle". We have been studying the carbon cycle of the Howland Forest in central Maine, an unmanaged evergreen forest with most trees between 100 and 200 years old. Over the last 25 years the forest has stored almost 3.5 tons of CO₂ per acre each year, even though that timespan has included the warmest, wettest, and driest years in the last 125. Although the forest is maturing, it is storing on average a bit more carbon each year and there is as yet no clear reason why. Forest growth is a natural solution to the problem of too much CO₂ in the atmosphere. This research helps show the longer-term stability and viability of forests as natural climate solutions.

1. Introduction

Understanding the movement and storage of carbon in forests and other natural systems has long been a central goal of ecology (Gosz et al., 1978; Whittaker et al., 1974). This understanding is complicated today by rapid changes in the climate, biochemical environment, and disturbance regime in which ecosystems operate. At the same time, natural systems can play prominent roles in absorbing atmospheric CO₂ and thus reducing the impacts of present and past emissions (Pan et al., 2011).

HOLLINGER ET AL. 1 of 21



Funding acquisition: D. Y. Hollinger, E. A. Davidson, A. D. Richardson, K. Savage

Investigation: D. Y. Hollinger, E. A. Davidson, S. Fraver, H. Hughes, J. T. Lee, A. D. Richardson, K. Savage, D. Sihi, A. Teets

Methodology: D. Y. Hollinger, E. A. Davidson, S. Fraver, H. Hughes, J. T. Lee, A. D. Richardson, K. Savage, D. Sihi A Teets

Project Administration: D. Y. Hollinger

Resources: D. Y. Hollinger, E. A. Davidson, S. Fraver, A. D. Richardson Software: D. Y. Hollinger, A. D. Richardson, K. Savage, D. Sihi, A. Teets Supervision: D. Y. Hollinger, E. A. Davidson, S. Fraver

Validation: D. Y. Hollinger, J. T. Lee, A. D. Richardson, K. Savage, D. Sihi, A. Teets

Visualization: D. Y. Hollinger, E. A. Davidson, S. Fraver, H. Hughes, A. D. Richardson, K. Savage, D. Sihi, A. Teets Writing – original draft: D. Y. Hollinger, E. A. Davidson, S. Fraver, A. D. Richardson, K. Savage, D. Sihi, A. Teets

Writing – review & editing: D. Y. Hollinger, E. A. Davidson, S. Fraver, A. D. Richardson, K. Savage, D. Sihi, Natural climate solutions (NCS) refer to a variety of land conservation and restoration actions that increase carbon storage (or reduce other greenhouse gas emissions) in forests and agricultural operations (Fargione et al., 2018; Griscom et al., 2017). Reforestation, extending forest harvest intervals, and avoiding conversion of forests or grasslands to other uses are all important natural climate solutions. Importantly, a useful NCS will maintain its carbon store long into the future ("permanence") even as the climate changes. Anderegg et al. (2020) discuss how climate-driven risks to carbon cycle processes and disturbance may compromise the permanence of forest-based natural climate solutions. Our research addresses the permanence of the Howland Forest carbon storage and the consistency of its annual C sink during the last 25–30 years.

Long term carbon flux monitoring sites and networks are ideal for evaluating potential natural climate solutions (Baldocchi & Penuelas, 2019; Hemes et al., 2021). Some of these sites now have over 2 decades of records of carbon flow into and out of an ecosystem as well as the meteorological, ecological, and biogeochemical measurements to put these fluxes in context. We report here average carbon pools and annual fluxes based on 25+ years of measurements carried out at the Howland Forest AmeriFlux site in central Maine, USA (Hollinger et al., 1999, 2004). This unmanaged, mixed-age forest is characterized by canopy trees 100–200 years old. The 25-year span of eddy flux measurements and 26-year span of inventory data represent a significant fraction of the life of the existing trees and are relevant to the issue of NCS permanence. These flux and inventory data are complemented by meteorological and environmental measurements, canopy leaf area index (LAI) and phenology, and component fluxes including soil respiration and litterfall.

The Howland Forest as an NCS is an example of "Improved forest management" or more specifically, an unmanaged "carbon reserve". The forest is owned by the Northeast Wilderness Trust, which has the goal of preserving the land as forever-wild. The forest was registered as a Climate Action Reserve (CAR681) in 2013 to provide carbon offset credits.

The Howland Forest has further matured since detailed measurements of whole-ecosystem CO_2 , water vapor, and energy fluxes at Howland began in 1996 (Hollinger et al., 1999). The climate in central Maine and the northeastern US over the last 25 years has been warmer and wetter than the long-term average (NOAA, 2021). Variability also appears to have increased. Over the 25 years of flux measurement, atmospheric CO_2 has increased from about 363 to ~413 ppm while tropospheric ozone levels, and sulfate and nitrate inputs have plummeted. During our measurements the region has experienced the hottest, driest, and wettest years in a record extending over 125 years (NOAA, 2021).

The goals of this work are similar to those expressed in a compatible, recently published study of C cycling at the Harvard forest (Finzi et al., 2020). These goals include quantifying the long-term C balance of a forest, as well as assessing the controls on variability and likely future of on-site carbon storage. Howland lies just over 400 km to the NE of the Harvard forest and shares a similar climate and several tree species. However, the Harvard forest is dominated by broadleaf deciduous species including red oak (*Quercus rubra*) and red maple (*Acer rubrum*) while Howland consists primarily of needle-leaf evergreens. Here we compare our multi-decadal records of C cycle processes in an evergreen forest with those from the climatically similar deciduous Harvard forest. We address several questions about aging forests and find that our longitudinal results support recent findings of different patterns of age-related resource use efficiency in evergreen and deciduous forests (Xu et al., 2020).

2. Materials and Methods

2.1. Site Description

The Howland Forest AmeriFlux site is located in central Maine, USA (45.2041°N 68.7402°W, elevation 60 m above sea level) on 550 acres of flat to gently rolling forestland owned by the Northeast Wilderness Trust. The mature multi-aged forest is about 90% conifer, dominated by red spruce (*Picea rubens*) and eastern hemlock (*Tsuga canadensis*), with lesser quantities of northern white cedar (*Thuja occidentalis*), balsam fir (*Abies balsamea*), and white pine (*Pinus strobus*). The ~10% deciduous tree species are mainly red maple (*Acer rubrum*), paper birch (*Betula papyrifera*), and yellow birch (*Betula alleghaniensis*). The site sits at the ecotone of the North American boreal spruce-fir zone. The dominant soils were formed in coarse-loamy granitic basal till and range from well drained to very poorly drained over relatively small areas (Levine et al., 1994). Wetland soils are Histosols and upland soils are fine sandy loams, classified as Aquic

HOLLINGER ET AL. 2 of 21



Haplorthods. The climate is damp and cool, with average annual temperatures of 6.2°C and a mean annual precipitation of 1148 mm (Daly et al., 2008). The site has evidence of previous logging (evenly distributed, well-decayed cut stumps) but has been unmanaged for roughly a century. Compared to other stands of the region, Howland Forest is diverse in both tree size and age distribution. The site supports several remnant trees in excess of 200 years old, along with many standing dead trees, and exhibits pit-and-mound topography. The climate, soils, and vegetation at the site are more fully documented in the AmeriFlux BADM (Biological, Ancillary, Disturbance and Metadata) record.

2.1.1. Ecological Measurements

Leaf area index (m^{-2} m^{-2}) was measured periodically (Richardson et al., 2011) within the tower footprint using a LAI 2000 plant canopy analyzer (Li-Cor Inc, Lincoln, NE). (Note that these measurements include branches and stems so are properly plant area index, PAI.) A 200 m transect, running in an N-S direction, was established 50 m north of tower US-Ho1 in 2006 and sampled in the middle of the summer in most subsequent years. Measurement points were established at 10 m intervals and marked with flags. Prior to 2006, LAI measurements were made across a larger number of more dispersed plots. We used the formulation of Chen et al. (2006) to estimate actual LAI from "effective" (measured) LAI, using clumping and other factors as described in Richardson et al. (2011).

Sampling uncertainties were estimated as the standard error of the mean LAI for each set of measurements (n=20 plots), typically $\approx 0.1 \text{ m}^2 \text{ m}^{-2}$. Systematic errors due to sensor cross-calibration were estimated, based on results from a more intensive LAI campaign at Howland (Richardson et al., 2011), to be $\approx 0.2 \text{ m}^2 \text{ m}^{-2}$. Random errors, evaluated by repeat measurements of the same transect, were sufficiently small for individual measurements ($1 \sigma = 0.15 \text{ m}^2 \text{ m}^{-2}$) that they could be ignored, given the number of plots sampled, and the other (larger) sources of uncertainty. Total uncertainty in stand-level LAI was thus estimated to be $0.3 \text{ m}^2 \text{ m}^{-2}$. LAI was converted to canopy mass based on a mean (across dominant conifer species) foliage mass-to-area ratio of 280 g dry foliage m⁻².

Field observations of springtime bud burst phenology have been conducted at Howland Forest since 1990 and are ongoing (Richardson et al., 2009). In spring, the mean aggregate (across the dominant species) dates of bud burst by coniferous (hemlock and red spruce) and deciduous (paper birch and red maple) species are estimated from observations made during weekly or twice-weekly site visits. In autumn, coloration and leaf drop (as percentages) of the deciduous species are visually estimated on a similar schedule. Here, we use 50% canopy coloration as our fall phenology metric.

Since 2008, phenology of coniferous and deciduous species has been tracked at Howland using two PhenoCams, howland1, and howland2, respectively (Richardson, 2019). Imagery, recorded every 30 min from sunrise to sunset, is processed to provide daily measures of canopy greenness, from which start- and end-of-season transition dates are extracted using established methods based on dates when the canopy greenness reaches (rising in spring, falling in autumn) 25% of the seasonal amplitude, where amplitude is calculated as the difference between the summer maximum and winter minimum (Richardson et al., 2018). For conifers, seasonal changes in canopy greenness are driven by leaf-level changes in pigmentation, specifically the carotenoids:chlorophyll ratio (Bowling et al., 2018; Seyednasrollah et al., 2021); in late winter and early spring, increases in canopy greenness occur independently of (and well in advance of) the production of new foliage. By comparison, for deciduous species, seasonal change in canopy greenness are driven by budburst and leaf expansion in spring, and leaf coloration and leaf fall in autumn. Start-of-season transition dates derived from PhenoCam imagery tend to lag slightly behind visual observations of deciduous budburst, while end-of-season transition dates tend to align with dates of peak autumn color.

2.1.2. Meteorological Measurements

Present meteorological measurements include air temperature at 2 and 30 m (shielded and ventilated platinum resistance thermometer), precipitation (heated tipping bucket rain gage, model TR-525; Texas Electronics), air pressure (model PTB100A analog barometer; Vaisala), incoming and outgoing shortwave and longwave radiation (model CNR4, Kipp & Zonen), total photosynthetically active radiation (model PAR Lite quantum sensor, Kipp & Zonen) and its direct and diffuse components (BF5 Sunshine Sensor, Delta T Devices) all sampled at 15 s intervals and averaged to 30 m. Wind speed and direction, as well as vapor pressure deficit and relative humidity are calculated from the eddy covariance data described below. Profiles of

HOLLINGER ET AL. 3 of 21



soil temperature and soil moisture are measured hourly (sensors are installed at depths of 5, 10, 20, 50, and 100 cm) using Hydra probes (Stevens Water Monitoring Systems Inc.), located near the base of the tower. Water table depth is measured in two shallow wells about 30 and 50 m from the tower using barometrically compensated pressure transducers (model WL400, Global Water).

Clean Air Status and Trends Network (CASTNET, https://www.epa.gov/castnet) measurements of atmospheric chemistry have been made at the Howland forest for many years (sites How132 and How191). These measurements of concentrations of gases and particles include SO_2 , nitric acid (HNO₃), sulfate (SO_4^{2-}), nitrate (NO_3^{-}), ammonium (NH_4^{+}), chloride (Cl^{-}), and base cations, as well as hourly O_3 concentrations. We show change in the ozone W126 index which weighs concentrations in a sigmoidal manner and sums day-time hourly concentrations. This index is designed to reflect cumulative exposures that can damage plants and trees during the consecutive three months in the growing season when daytime ozone concentrations are the highest and plant growth is most likely to be affected (Musselman et al., 2006).

 CO_2 dry air mole fraction is measured in the airstream pulled from the top of the tower as part of the eddy covariance flux system. The use of a high precision low drift gas analyzer since 2011 (see below) allows comparison of Howland with Mauna Loa or other measurement stations. Monthly values were calculated from midday (1000–1500) half-hourly measurements that passed the quality criteria in Richardson et al. (2019).

2.2. Forest Flux Measurements

2.2.1. Whole Ecosystem Eddy Covariance Fluxes

Continuous measurements of CO2, H2O, and energy flux using the eddy covariance technique began at the main Howland tower (US-Ho1) in late 1995. The measurement systems have been fully described previously (Hollinger et al., 1999, 2004) along with important updated details of processing (Richardson et al., 2019). Our philosophy has been to minimize changes in the physical measurement systems and software algorithms. Fluxes have been measured at a height of 31 m with an instrument system consisting of a model SAT-211/3K 3-axis sonic anemometer (Applied Technologies Inc.) and fast-response closed-path CO₂/H₂O analyzers. From 1996 to mid-2011 model LI6262 analyzers (LI-COR Biosciences) were used and several instruments were rotated through as necessary for calibration, maintenance, and repair. In mid-2011 this was replaced with a model LI7200 analyzer and, in parallel, a CO₂/H₂O/CH₄ cavity ring-down spectrometer (model G2311-f, Picarro Inc.). Sampled air was pulled from the top of the tower through a 0.2 micron PTFE capsule filter with one end severed and ~46 m of 4.8 mm (inner diameter) LLDPE (U.S. Plastics Corp.) at a nominal flow rate of 4.5 standard liters per minute. The tubing and filter were replaced annually. All data, including concentrations of H₂O and CO₂ reported as dry air mole fractions were recorded at 5 Hz on a PC until 2011 and then via data logger (model CR1000, Campbell Scientific Inc.). CH₄ fluxes have also been measured on the main Howland tower using the eddy covariance method since 2011 (Richardson et al., 2019; Shoemaker et al., 2014) but are not reported here.

Raw, high-frequency data were converted in our original system to 30-min fluxes using the flux software of McMillen (1988). Processing later switched to using EddyPro* Eddy Covariance Processing Software (LI-COR Biosciences). For this study we re-processed the entire 25-year flux data record using EddyPro version 6.2.2. We calculated turbulent fluxes of CO_2 as well as sensible (H) and latent (LE) heat flux using the custom EddyPro settings described in Richardson et al. (2019). To estimate the u* (friction velocity) threshold for nocturnal values, fill gaps in the record, and estimate annual net ecosystem exchange (NEE) as well as gross primary production (GPP) and ecosystem respiration ($R_{\rm eco}$), we used the R package "REddyProc" version 1.2.2 (Wutzler et al., 2018) with RStudio, Version 1.3.1073 and R version 4.0.2.

2.2.2. Uncertainty Estimates of Fluxes

For each half-hour CO₂ flux value, we calculated uncertainties using the method of Finkelstein and Sims (2001) as implemented in EddyPro version 6.2.2. For calculating annual uncertainties we used the Monte Carlo method and sampled the exponential distribution based on the associated half-hourly uncertainty calculated by EddyPro to create 20 samples of each half-hourly value in each year. This yielded 20 separate annual flux datasets with gaps that were processed by REddyProc and used to estimate annual

HOLLINGER ET AL. 4 of 21

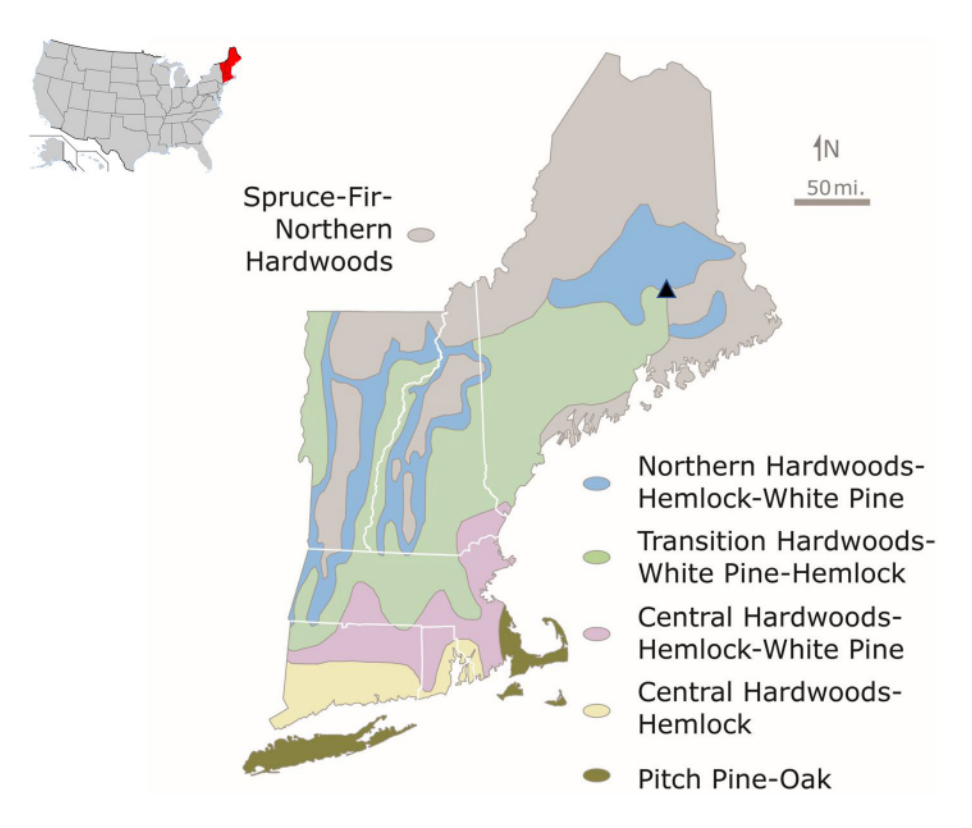


Figure 1. The Howland Forest (triangle, $45.2041^{\circ}N$ $68.7402^{\circ}W$) is located in central Maine, USA in the ecotone between temperate deciduous and boreal forests.

mean C fluxes and standard deviations. In this way, measurement uncertainties are correctly propagated all the way through gap filling (e.g., Richardson & Hollinger, 2007).

2.2.3. Flux Footprint Analyses

To calculate the flux source (footprint) regions and place our inventory measurements in spatial context with the eddy fluxes, we used the 2-D flux footprint parameterization of a stochastic particle dispersion model from Kljun et al. (2015). (See https://geography.swansea.ac.uk/nkljun/ffp/www/index.php for a useful on-line implementation). Because nocturnal and daytime stability differ strongly and influence the size of the footprint, we calculated separate night and day footprints using half-hour data from 2000 to 2019.

2.2.4. Soil Respiration Including Partitioning

Soil respiration, an important component of total respiration, was manually measured near the tower (Figure 2) during daylight hours from 1996 to 2012 using a system described by Savage and Davidson (2001). Typically, measurements were made once per week during the growing season (May–September) and one to two times per month during the late autumn, winter, and early spring. At each plot, eight permanent collars, 25 cm in diameter and made from thin wall PVC tubing cut to 10 cm lengths, were inserted into the ground to a depth of \sim 5 cm.

Automated flux measurements were made from 2004 to 2016 following the methods described previously (Richardson et al., 2019; Savage & Davidson, 2003). Three to six opaque chambers were sampled for 5–15 min once every 30–120 min for automated flux measurements, with the frequency varying because of different research objectives which varied over the 12 study years.

We used a classical root trenching experiment during 2013–2015 at the Howland Forest (Carbone et al., 2016) to partition soil R into its autotrophic (R_a) and heterotrophic (R_h) components where the trench plot fluxes provide data for R_h and the difference between trenched and untrenched (control) plots provide constraints for root respiration (i.e., R_a). Partitioning was also estimated using radiocarbon measurements of soil CO_2

HOLLINGER ET AL. 5 of 21

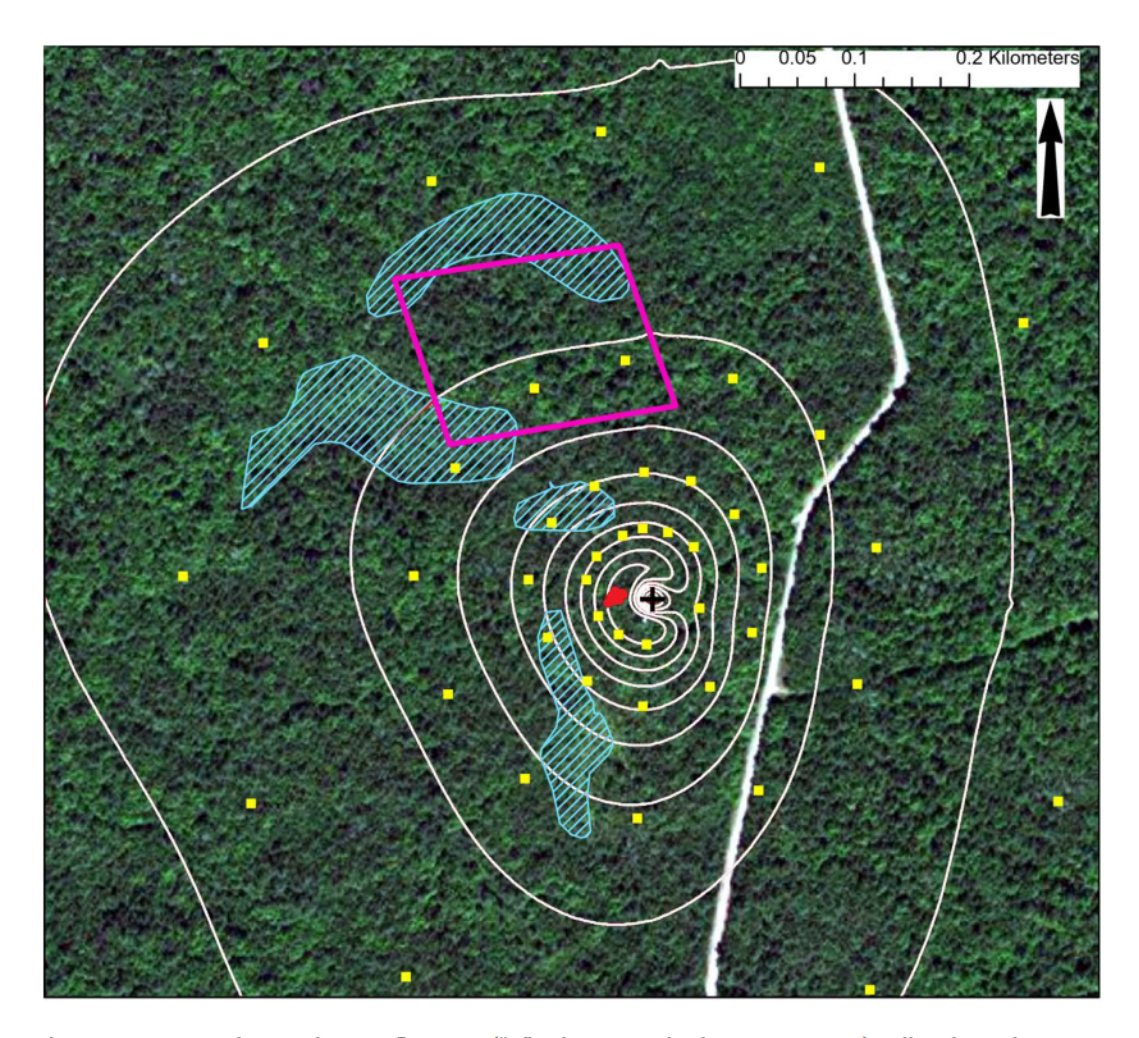


Figure 2. Inventory plots in relation to flux tower ("+" indicates Howland Main tower, Ho1). Yellow dots indicate inventory plots and purple the NASA megaplot. The red overlapping dots show soil respiration locations. Stippled areas indicate slightly lower elevation (wetter) areas. The thin white lines indicate average daytime flux 10-90 percentile isopleths. The heavy white line is the access road. Image about 1×1 km.

emissions. For this analysis, we use the average partitioning coefficients of the two approaches reported by Carbone et al. (2016). Triplicate trenches were dug by excavating soils from 1-m depth covering an area of 3×3 m. The trench was then lined with a plastic wrap to prevent root growth back into the plots, and the soil layers were carefully backfilled. An automated chamber was installed in each trenched and untrenched plot.

2.2.5. Leaf Litter and Other Transfers

Litterfall (foliage and fine twigs) was estimated by collection of the contents of baskets (8 baskets per plot) twice per year (late fall and early spring), with data aggregated to annual (autumn-to-autumn) estimates. These data are used to calculate total belowground carbon allocation as described later. Sampling errors were calculated as the standard error of the annual litterfall across the n = 8 samples, and ranged from 10%-30%.

2.3. Forest Biomass Inventories

Net primary production in living trees was estimated using two long-term plot-based inventories. Whole-tree biomass (including leaves and coarse roots) was estimated using species-specific allometric equations (Young et al., 1980) from DBH measurements of all trees ≥ 10 cm on n = 44 inventory plots, and for the

HOLLINGER ET AL. 6 of 21



n=48 subplots (25 \times 25 m) in the 3-ha megaplot. The dry mass estimates produced from the allometric equations were converted to carbon mass by multiplying by species-specific carbon ratios (Lamlom & Savidge, 2003). The uncertainty of the annual net primary production was estimated using 1000 Monte Carlo simulations of net primary productivity at the plot-level for the inventory set and megaplot individually. The carbon pool stored in living tree biomass was estimated using the 3-ha megaplot.

2.3.1. Megaplot

The megaplot is a large stem-mapped plot (3 hectares; 150×200 m) used here to obtain annual estimates of biomass C increment. It was established in 1989 by the Laboratory for Terrestrial Physics at NASA's Goddard Space Flight Center (see Levine et al., 1994; Ranson et al., 2001; Sun et al., 2011; Weishampel et al., 1994) and located 240 m north of the flux tower (Figure 2). In this plot, all trees greater than 3.0 cm diameter at breast height (DBH, 1.37 m) were mapped and measured, recording ca. 7,800 stems. In 2015, all trees greater than 10.0 cm were inventoried and measured. The tree species composition of this megaplot is nearly identical to that of continuous forest inventory plots surrounding the tower (Hollinger et al., 2004). The plot has been the focus of recent work on Howland forest productivity (Fien et al., 2019; Teets, Fraver, Hollinger, et al., 2018a; Teets, Fraver, Weiskittel, & Hollinger, 2018b).

Net primary production in trees was estimated with annual resolution in the megaplot from 1989 to 2015 using a 10% subset of the trees. The subset was selected in a random stratified manner (by species and diameter class), resulting in 327 trees. One increment core was extracted from each tree at breast height with a standard 5.2 mm increment borer (Häglof Company Group), and ring-widths were measured to the nearest 0.01 mm using a Velmex sliding stage (Velmex Inc.) with MeasureJ2X software (VoorTech Consulting). Cross-dating was performed using marker years, usually light or narrow rings, followed by statistical cross-dating using COFECHA software (Holmes, 1983). Ring widths were estimated for the remaining trees in the megaplot by scaling cored-tree data to the plot-level based on the assumption that the randomly selected cored trees adequately represent the entire tree population (see Teets, Fraver, Hollinger, et al., 2018).

2.3.2. Inventory Plots

Inventory plots, located along 30° radial transects at distances of 50, 100, 200, and 400 m from the tower, were established in 2001 and inventoried and measured every 2–3 years. Each circular plot had a radius of 7.3 m (identical to USFS Forest Inventory and Analysis [FIA] subplots), and all trees greater than or equal to 10 cm were measured. Two of these plots fell on areas cleared for roads, and two of the plots were missing data for one of the sampling periods and were excluded. The total number of plots used for this analysis was n = 44.

Standing biomass was estimated for all plots at each year of measurement—2001, 2003, 2005, 2007, 2009, 2012, 2015, and 2018. The difference in standing biomass between inventories was estimated and converted to the average annual growth between sampling periods. Trees that died, or trees with equal or slightly smaller current diameters than those recorded in previous inventories were assumed to have zero growth, and therefore no increase or decrease in carbon mass. Ingrowth was assumed to have the minimum diameter (10 cm) for all previous inventories, therefore only growth of trees greater than 10 cm contributed to annual net primary production.

2.3.3. Deadwood

The inventory of all deadwood components (coarse and fine woody debris, standing dead trees and saplings, and stumps) was conducted on the megaplot between 2015 and 2017. Downed coarse woody debris (CWD, pieces >10 cm diameter) and fine woody debris (FWD, pieces <10 cm) volumes were estimated using the line-intersect method (van Wagner, 1968). Stump volumes were calculated from field measurements, assuming the form of a cylinder. Volumes of CWD, FWD, and stumps were converted to mass using species- and decay-class specific densities (Harmon et al., 2008). Mass of standing dead trees (snags) and dead saplings was calculated using species-specific, whole-tree allometric equations developed for this region (Young et al., 1980), based on megaplot re-inventories conducted in 2015 (trees) and 2017 (saplings).

HOLLINGER ET AL. 7 of 21



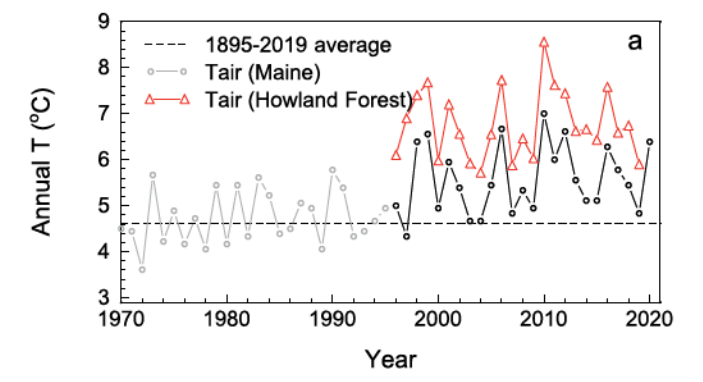
Mass of all deadwood components was converted to carbon mass assuming carbon content of 50%. Standard errors around these estimates were determined by repeatedly (100 times) concatenating randomly selected transect segments (CWD, FWD) or by repeatedly (100 times) resampling the complete plot inventory data (snags, saplings, stumps). (See Supporting Information for more detail.)

Annual flux rates for all the above deadwood components were estimated from published species-specific decay constants (Russell et al., 2014) applied to our estimated carbon mass. Standard errors for each flux rate were estimated using 100 Monte Carlo simulations of the published variance (Russell et al., 2014).

3. Data

3.1. Data Availability

The Howland Forest is a core AmeriFlux site. Eddy flux and meteorological data are available through the AmeriFlux data system (https://ameriflux.lbl.gov/). Additional Biological, Ancillary, Disturbance, and Metadata (BADM), non-continuous information and data that describe and compliment the flux and meteorological data are available from the same location. Gap-filled flux data, soil respiration data, inventory measurements, LAI, phenology, and litterfall, are available from the USDA Forest Service Research Data Archive (https://doi.org/10.2737/RDS-2021-0014). PhenoCam imagery and derived data are publicly available in real time (https://phenocam.sr.unh.edu) and are also archived at the ORNL DAAC (https://daac.ornl.gov/cgi-bin/dsviewer.pl?ds_id=1689).



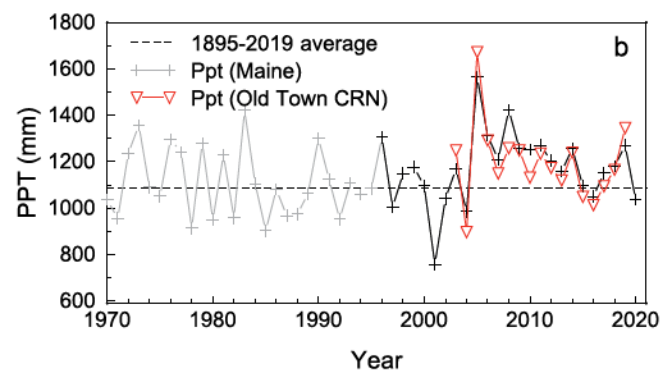


Figure 3. Average annual temperatures in central Maine have risen since record keeping began in 1895 and during the flux measurement period have averaged about 1.4°C above the long-term average (a). The flux record at Howland incorporates the wettest (2005) and driest (2001) years on record (b).

4. Results

4.1. Climate Trends at the Howland Forest

The Howland Forest and Maine have experienced a long-term annual warming trend while winter months are becoming wetter (Kunkel et al., 2013). Since 1970, for example, the mean annual temperature across Maine has been rising about 0.28°C per decade (Figure 3a). By contrast, there is no trend in annual total precipitation over the same period (Figure 3b). Mean annual temperature and precipitation in the region over the study period (1996-2020) are marked by high variability. The mean values for the state of Maine are representative of conditions at Howland (located roughly mid-state) and can be used to put recent conditions into a longer-term perspective. Since 1996, tower-based annual temperature has varied in concert with statewide values ($r^2 = 0.79$, P < 0.001, Figure 3a) but averaged ~1.2°C higher. Much of this offset is likely a consequence of the measurement location above a forest canopy in comparison to the near-surface recordings of NOAA stations. Lee et al. (2011) found surface air temperature lower in open land than above nearby forested land by about 0.85°C northwards of 45°N. Precipitation is difficult to measure at Howland as there are few gaps suitable for shielded precipitation collectors. The Old Town NOAA Climate Reference Network (CRN) station is located within 40 km and has records back to 2002. Annual precipitation at the Old Town site is correlated with the statewide average ($r^2 = 0.84$, P < 0.001, Figure 3b).

Long-term records (dating from 1895) suggest conditions have been warmer and wetter than the 125-year average since measurements began at Howland. This is relevant to forest growth since the majority of canopy trees were established prior to 1895. Each of the last 25 years in central Maine (except 1997) has been warmer than the long-term average (Figure 3a). The Howland tower flux record encompasses the seven warmest years recorded since 1895. Similarly, 19 of the last 25 years have been

HOLLINGER ET AL. 8 of 21



wetter than the long-term average (Figure 3b). The flux record encompasses both the wettest (2005) and driest (2001) years for Maine over the last 125 years.

4.2. Changes in Atmospheric Chemistry and Deposition

Nitrogen and sulfur deposition at Howland have declined from the early 2000s as tighter regulations in the Clean Air Act came into force (Figure 4a). The decline in sulfur wet + dry deposition $(0.024 \pm 0.006 \text{ g m}^{-2} \text{ y}^{-1})$, mean slope and 95% confidence interval) has been about twice that of nitrogen deposition $(0.011 \pm 0.003 \text{ g m}^{-2} \text{ y}^{-1})$. Ground-level ozone concentrations (Figure 4b), especially when weighed for phytotoxicity, have declined even more dramatically and appear to have leveled off at \sim 20% of values in the late 1990s. The phytotoxic impacts of ozone are non-linear and cumulative (Felzer et al., 2007; Schmieden & Wild, 1995).

 CO_2 concentrations at Howland broadly follow the global trend as shown at Mauna Loa (now 2.5 ppm y⁻¹). However, the annual amplitude of monthly averaged atmospheric CO_2 at Howland is influenced by local and regional sinks (vegetation photosynthesis) in the summer and sources in the winter (fossil fuel emissions and ecosystem respiration). The annual amplitude of Howland Forest midday CO_2 measured at 30 m (about 10 m above the forest canopy) is about 4 times that at Mauna Loa which represents variation in the free troposphere (Figure 4c). The relative increase of atmospheric CO_2 over the flux measurement record (~14%) is smaller than the changes in pollutants over the same time period.

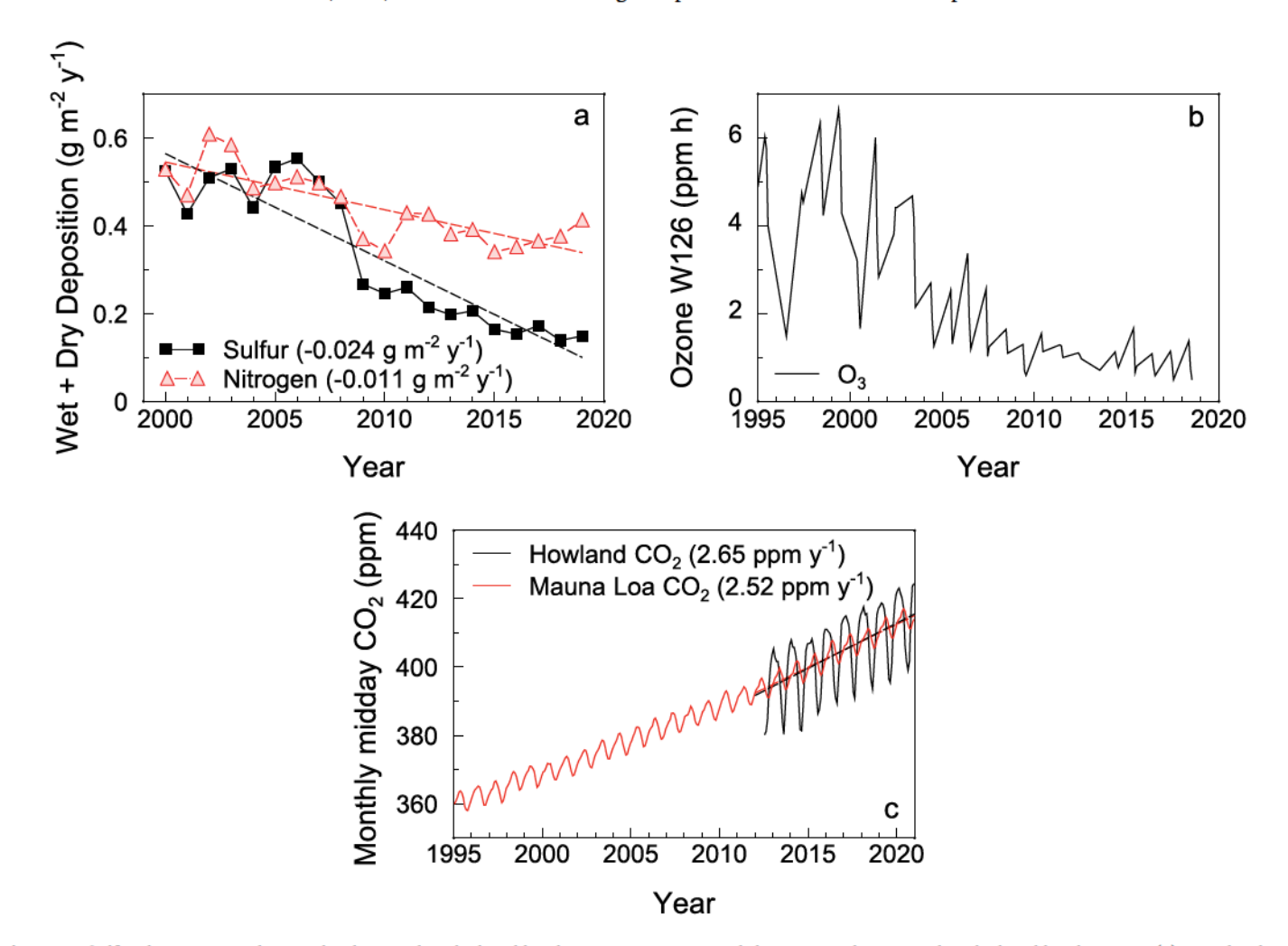


Figure 4. Sulfur deposition at the Howland Forest has declined by about 68% since 2000 while nitrogen deposition has declined by about 30% (a). Weighted, summer ground-level ozone has declined by over 80% (b). Midday mean annual CO₂ concentration at Howland Forest closely follows values recorded at Mauna Loa (data courtesy NOAA Global Monitoring Laboratory) and have likely risen about 14% since 1996 (c).

HOLLINGER ET AL. 9 of 21



Table 1
Contemporary C Stocks at the Howland Research Forest

Component	Stock (±SD)	Source	
Living			
Whole trees	10600 ± 2900	Megaplot	
Whole trees	14500 ± 4900 Inventory plots		
Saplings	290 ± 4	Megaplot	
Dead			
Whole trees	440 ± 20	Megaplot	
Saplings	100 ± 3	Megaplot	
Coarse Woody Debris	410 ± 70	Megaplot	
Fine Woody Debris	210 ± 30	Megaplot	
Stumps	90 ± 4	Megaplot	
Soils			
Forest Floor	4400 ± 1800	4400 ± 1800 Fernandez et al., 1993	
Mineral soil	$6,700 \pm 2900$	Fernandez et al., 1993	
Total (megaplot)	23300 ± 4200		

Note. Units in g C ${\rm m}^{-2}$; megaplot (except saplings) and FIA-like plot inventory data from 2015; saplings inventoried 2017.

4.3. Flux Footprint and Biomass Sampling Locations

 $\rm CO_2$ flux footprint modeling (Figure 2) suggests that during the daytime, about 50% of the measured $\rm CO_2$ uptake originates within about 90 m of the tower (\sim 2.5 ha) while 90% occurs within about 320–420 m of the tower (\sim 50 ha). The region of forest with the most influence on the fluxes occurs between about 40 and 90 m from the tower. At night, more stable conditions increase the effective source area so that the 50% distance increases to \sim 130 m (\sim 5 ha). At night the 90% source region extends out to about 500 m to the east of the tower and to over 900 m to the northwest. This means that the $\rm R_{eco}$ measurements that are based off nocturnal flux data come from a larger and more diffuse region than the daytime NEE measurements. All of our biomass inventory, soil respiration, litterfall and other measurements come from within \sim 400 m of the tower and are thus mostly (day) or totally (night) incorporated within the 90% flux footprint regions. The megaplot lies between about 200 and 350 m of the tower.

4.4. Carbon Stocks

Total ecosystem C stock determined from the megaplot and nearby quantitative soil pits was 23,300 g C m $^{-2}$ (Table 1). Of this total, 46% was in live trees, and ca. 1% in live saplings. Soil (forest floor plus mineral soil to a depth of 80 cm) represented 48%; all deadwood components combined represented only ca. 5% of total ecosystem C.

4.5. Tree Biomass Increment

Our estimates of annual biomass increment in trees at Howland Forest averaged 161 ± 23 g C m⁻² yr⁻¹ across different sampling techniques. Estimates from repeat diameter measurements in the inventory plots yielded similar estimates of biomass increment as those from the tree-ring analysis of the megaplot trees (Figure 5). The difference in the magnitude of biomass increment between the inventory plots and megaplot is thought to be driven by the larger trees in the inventory plots compared to the megaplot. We found that biomass increment estimated from remeasurements every 2–3 years in the inventory plots had high-

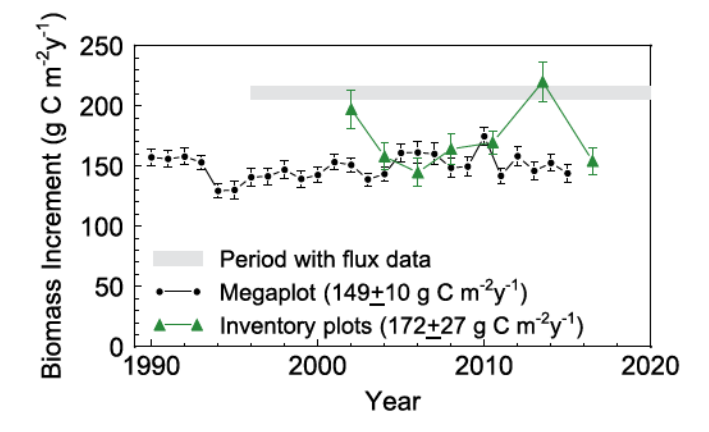


Figure 5. Annual tree biomass increment at Howland Forest based on repeat diameter measurements of inventory plots (green triangles), and a tree-ring analysis of a 10% subsample of trees in the megaplot (black circles). Dry biomass was estimated using the regionally derived allometric equations from Young et al. (1980) and converted to carbon mass (Lamlom & Savidge, 2003).

er variability and higher uncertainty compared to estimates using treering methodologies. For the period coincident with the flux tower record (1996–2015) the megaplot record indicated a non-significant trend in C uptake (0.6 \pm 0.7 g C m $^{-2}$ yr $^{-1}$, P=0.12). Estimates of biomass increment based on tree-ring analyses in the megaplot produced an annual time-series that demonstrates a resistance to change, based on a low interannual variability and high autocorrelation between years.

4.6. Phenology Changes

Ground observations of phenology (Figure 6) show that on average, budbreak by the deciduous species occurs on May 3 (day 123), more than 3 weeks ahead of the evergreen conifers (May 28); 50% autumn color is reached, on average, on October 9. Interannual variation (1 SD) in phenology is about ± 1 week for all measures. Although deciduous budbreak is trending later (0.25 d/y), this pattern is not statistically significant (P = 0.07) and appears to be mostly driven by the late budbreak in 2019 (P = 0.20 if this year is excluded).

PhenoCam-derived (2010-onwards) metrics for start- and end-of-season, which have been shown to be correlated with the onset and cessation

HOLLINGER ET AL. 10 of 21

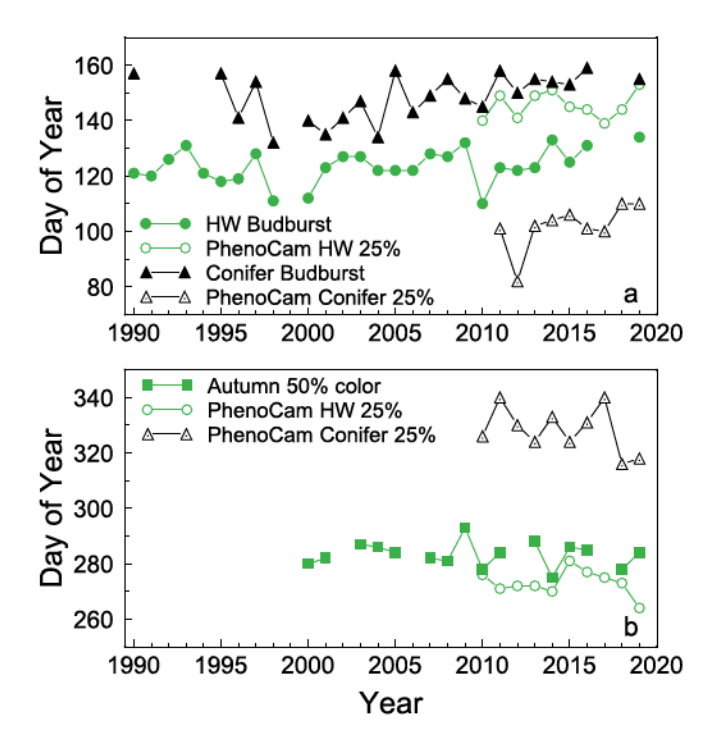


Figure 6. Field (solid symbols) and digital camera ("PhenoCam", open symbols) observations of Howland Forest phenology. "HW" refer to deciduous hardwood species.

of evergreen photosynthesis (Seyednasrollah et al., 2019, 2021), are also highly variable from year-to-year. The mean start-of-season date for the evergreens is April 11, although in 2012 start-of-season occurred almost 3 weeks earlier (March 23). The mean end-of-season date is November 23. "Green season length," calculated as the number of days between start- and end-of-season, averages 227 ± 14 (mean ± 1 SD) days, and was more than a month longer in 2011, 2012, and 2017 than in 2018 or 2019.

4.7. Leaf Area Index

LAI at Howland (as mentioned earlier, strictly "Plant Area Index") has averaged 5.8 \pm 0.5 m² m $^{-2}$. However, LAI has increased through time at a rate of ~0.05 m² m $^{-2}$ y $^{-1}$ (P < 0.01) (Figure 7). Based on a leaf mass per unit area (LMA) of 280 g m $^{-2}$ and a 50% C content, the increasing LAI represents a "sink" of ~7 \pm 4 g C m $^{-2}$ y $^{-1}$. The allometric equations we used for estimating biomass of the component species (Young et al., 1980) project an increase in foliage C mass of 10.5 g C m $^{-2}$ y $^{-1}$ based on the increase in tree size observed over time at the site, thus the sink associated with LAI increase is already accounted for in the allometry used to calculate change in biomass.

4.8. Whole Ecosystem Fluxes

The Howland Forest was a net sink for atmospheric CO_2 in each of the 25 years of measurement (Figure 8a). Annual net ecosystem production (NEP = -NEE) averaged over that interval was 211 \pm 40 g C m⁻² y⁻¹. Annual NEP varied 2-fold during the study, ranging between about

140 and 280 g C m⁻² yr⁻¹. There was a small but significant trend in NEP (slope = 2.4 ± 2.1 g C m⁻² y⁻¹, P = 0.025) over the measurement period indicating a gradual increase in net C uptake. GPP and R_{eco} averaged 1331 \pm 83 and 1127 \pm 90 g C m⁻² y⁻¹ (Figure 8b). There were significant decreasing trends in both of these variables over the measurement period. GPP declined by about 5.8 ± 4.2 g C m⁻² yr⁻¹ (P = 0.01), while R_{eco} dropped by 8.2 ± 4.3 g C m⁻² yr⁻¹ (P < 0.001). Thus, the apparent increase in C storage occurred despite GPP decreasing over the course of the study. This happened because respiratory losses (R_{eco}) declined more quickly than GPP, increasing the ratio of R_{eco} to GPP with time.

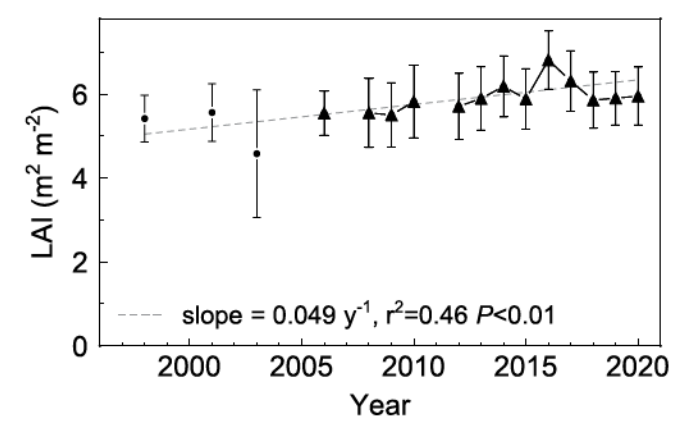


Figure 7. Leaf Area Index measured at Howland via LAI-2000 Plant Canopy Analyzer. Values prior to 2005 (circles) were from measurements conducted at the inventory plot locations (n=48). Since 2006, measurements were made at 10 m interval along a fixed transect to the NW of the tower (triangles). The slope of the increase obtained from the transect remeasurements (2006–2020) is not significantly different from that of all data shown here.

There were no significant temporal trends (Figure 9) in the long term measurements of soil respiration (slope = +7.7 g C m $^{-2}$ y $^{-1}$, P=0.06) or fine litterfall (slope = +1.5 g C m $^{-2}$ y $^{-1}$, P=0.08). The non-significant trend in soil respiration suggests that the drop in $R_{\rm eco}$ was likely due to the decline of aboveground autotrophic respiration, although uncertainties in both $R_{\rm eco}$ and soil respiration preclude making a strong inference about changes in aboveground respiration. The difference between soil respiration and fine litterfall (i.e., total belowground carbon allocation, TBCA, Davidson et al., 2002) also showed no temporal trend over the measurement period (1998–2016). Overall, annual soil respiration, fine litterfall, and TBCA averaged 816 \pm 108, 167 \pm 23, and 649 \pm 111 g C m $^{-2}$ yr $^{-1}$, respectively.

4.9. Monthly Trends

Small but significant trends were detected in the annual integrals of GPP, NEP, and ecosystem respiration. However, trends at annual scales may be difficult to identify due to interannual variability in the responses of carbon exchange to the environment and the fact that the annual val-

HOLLINGER ET AL. 11 of 21

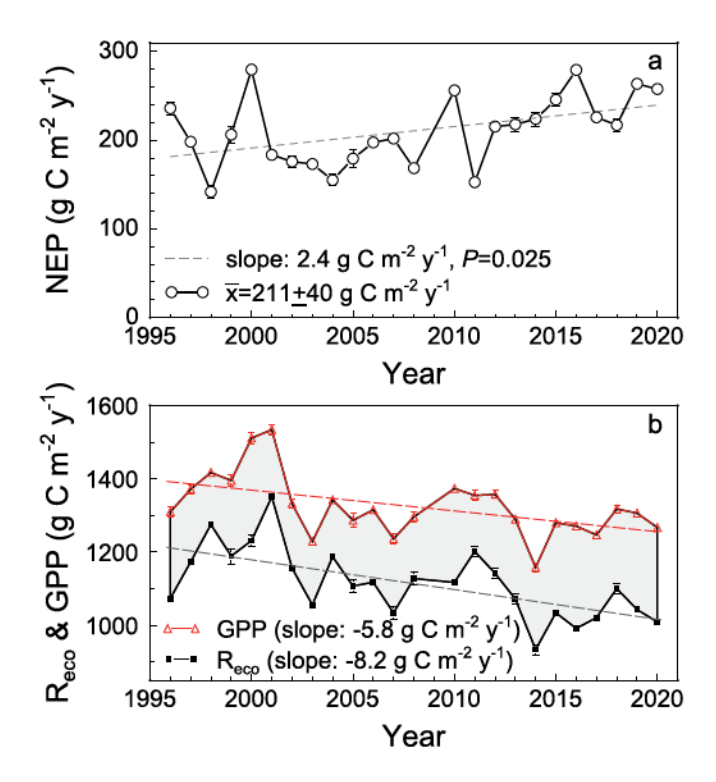


Figure 8. Annual carbon uptake measured by the eddy flux tower has averaged 211 g m $^{-2}$ at the Howland Forest (a). Both gross primary production (GPP) and ecosystem respiration have declined over time with $R_{\rm eco}$ declining more quickly than the decrease in GPP (b), leading to a small but significant increase in net ecosystem production (NEP; the widening between the dashed lines).

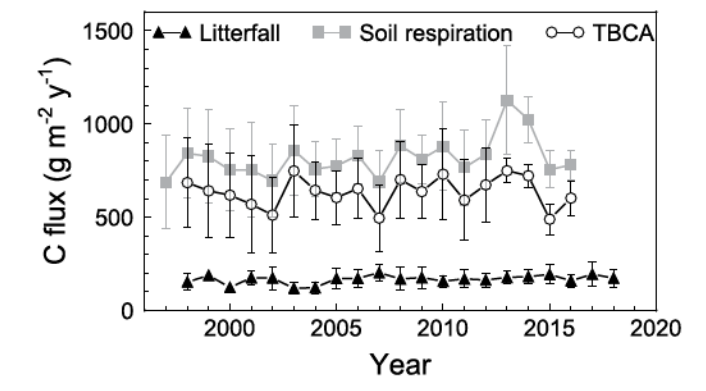


Figure 9. Soil respiration, fine litterfall, and total belowground carbon allocation at Howland Forest. Soil respiration was measured using LI-COR IRGA equipped with manual and automated chambers. Fine litterfall was measured using litter baskets. Total belowground carbon allocation was calculated following Davidson et al. (2002) assuming that soil C stocks are at quasi steady state.

ues represent integrals of a continuous process. Patterns in one part of a season which lead to enhanced uptake (such as an early spring) may be counterbalanced by below average C uptake later in the same year. We analyzed monthly variations in the eddy covariance data to determine if certain periods of the year are driving the interannual variation measured for GPP, NEP, and ecosystem respiration (Figure 10). The small decreases in annual GPP are due to declines in spring and summer productivity, with small but significant declines in April, June, and August over the sampling period. However, decreases in GPP are offset by ecosystem respiration declines in the summer and fall, resulting in slight increases in September NEP. Small yet significant decreases in winter $R_{\rm eco}$ are also contributing to modest increasing annual NEP over the sampling period.

The relationships between monthly temperature and ecosystem carbon exchange (i.e., GPP, NEP, and ecosystem respiration) were also tested to determine whether the effects of increasing temperature could affect the rates of carbon exchange differently throughout the year. We expected spring and winter carbon exchange to be positively related to temperature because of known temperature-limitations on photosynthesis of high latitude forests (Liu et al., 2020; Tanja et al., 2003). In the summer, we expected GPP and NEP to be negatively correlated with temperature because photosynthesis of the dominant species (Picea rubens) is known to be sensitive to high temperatures and possible water stress (Day, 2000; Vann et al., 1994). We found that GPP had largely positive correlations with temperature in the spring, whereas ecosystem respiration was positively correlated with temperature through most of the growing season (Figure 11). Although we did not find the expected negative effects of temperature on summer GPP, the positive correlations observed for spring months ceased, indicating that higher summer temperature did not enhance summer GPP. The net effect of these monthly variable responses of GPP and ecosystem respiration to temperature was a positive correlation between temperature and NEP in the early spring and a negative correlation in the late summer and autumn (Figure 11).

5. Discussion

5.1. Forest Biomass

The Howland Forest total C stock (23,300 \pm 4,200 g C m⁻²) is similar to old-growth softwood forests of the region (26,700 \pm 2,400 g C m⁻²; Hoover et al., 2012) and to a nearby *Picea rubens* forest (24,700 g C m⁻²; Puhlick et al., 2016) at the Penobscot Experimental Forest, 40 km to the south. But compared to two regional stands at the Harvard Forest, Howland Forest has considerably lower standing biomass. Finzi et al. (2020) found that a *Tsuga canadensis* stand at Harvard Forest contained 34,600 \pm 5,400 g C m⁻² and that the hardwood stand surrounding the EMS tower contained 29,600 \pm 4,700 g C m⁻². At the Harvard Forest 50% of the carbon in the *Tsuga* stand and 49% in the hardwood stand was contained in tree biomass and 44% was in soils. At Howland (using the megaplot inventory), we found similar results; tree biomass accounted for 45% of total C while soils held about 48%.

5.2. Forest Flux

The mean annual carbon uptake measured at Howland (211 g m $^{-2}$ y $^{-1}$) is comparable to previous studies of somewhat similar forests; however,

HOLLINGER ET AL. 12 of 21

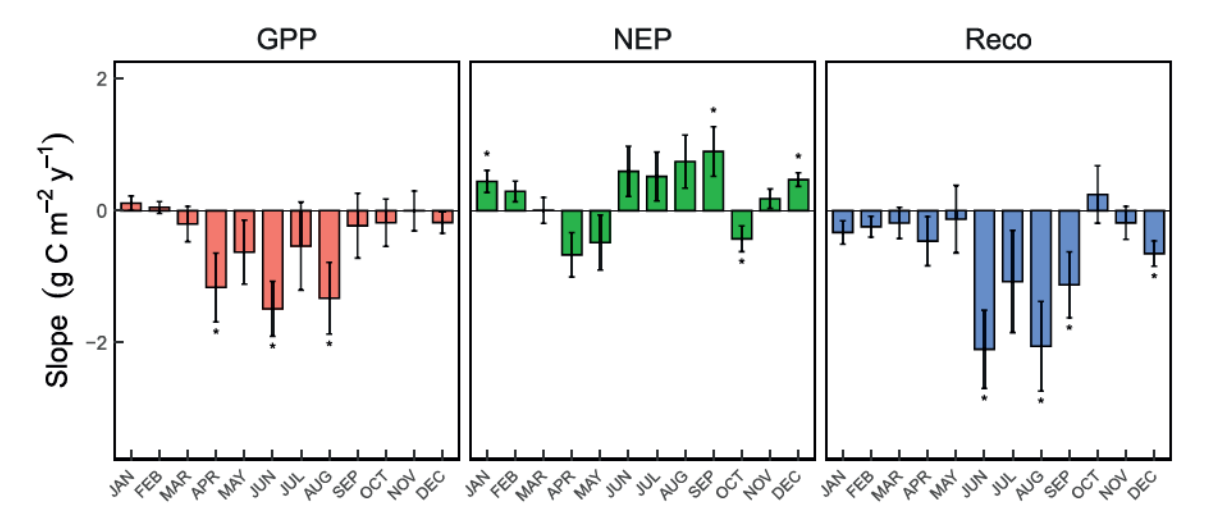


Figure 10. Slope of the trends in monthly integrals in ecosystem fluxes over the 25 years of observation. Positive slopes indicate months with increasing trends over the sampling period. Significant monthly trends are indicated with a "*".

the range of published values varies greatly. Of those long-term studies reviewed by Baldocchi et al. (2018), we select for comparison the conifer (or mixed deciduous-conifer) forests in the northern temperate or boreal region with stand ages greater than 75 years (but record lengths of 10 years or less). NEP from these studies ranges from -123 (a net carbon source) (Ricciuto et al., 2008) to 550 g C m⁻² y⁻¹ (carbon sink) (Grünwald & Bernhofer, 2007). We note that the inter-annual variability in NEP of our current study (SD \pm 40 g C m⁻² y⁻¹) is lower than any of these selected studies, which range from \pm 42 (Ricciuto et al., 2008) to \pm 221 g C m⁻² y⁻¹ (Carrara et al., 2003), and is consistent with the observation that high latitude conifer forests have lower inter-annual variability than do broadleaved forests (Baldocchi et al., 2018). Across the broad range of forest sites in the global Fluxnet database, Baldocchi (2020) found a mean annual uptake of 180 ± 243 g C m⁻² y⁻¹.

The Howland average annual flux over 25 years is about 70% of that measured above the Harvard Forest deciduous hardwood stand over 24 years. It is less than half that measured above the Harvard Forest hemlock stand (over 8 years) prior to an outbreak of the invasive insect pest, hemlock wooly adelgid (Finzi et al., 2020). Howland and Harvard share the same general climate but $\rm CO_2$ fluxes at Harvard appear more prone to disturbance than at Howland. At Howland, mean annual NEP and biomass increment

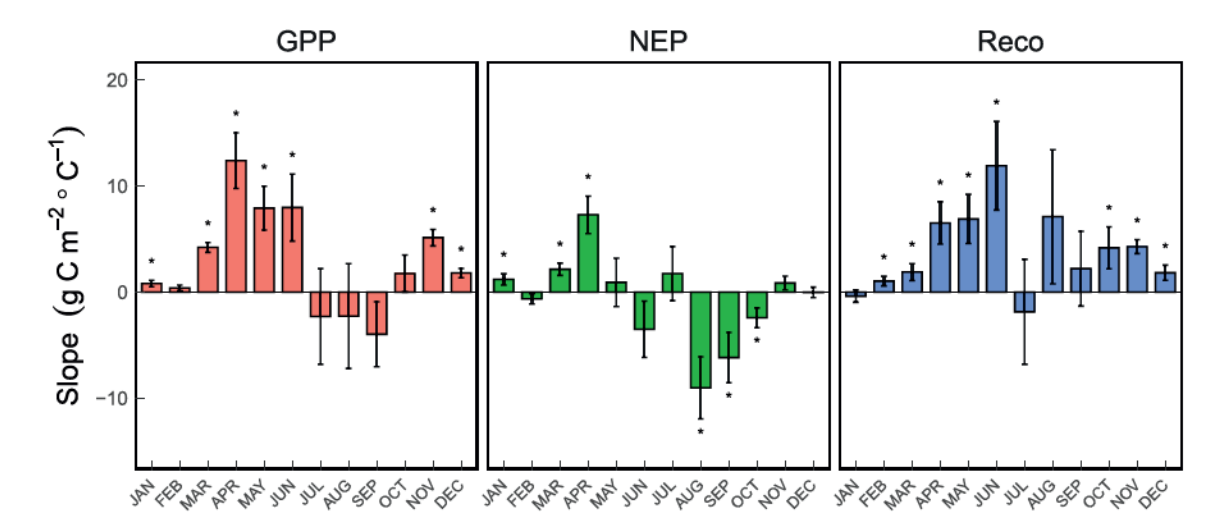


Figure 11. Slope of the relationship between ecosystem fluxes and temperature over the 25 years of observation. Positive slopes indicate months with increasing trends over the sampling period. Significant monthly trends are indicated with a "*".

HOLLINGER ET AL. 13 of 21



(161 g m $^{-2}$ y $^{-1}$) measurements agree to within about 50 g C m $^{-2}$ y $^{-1}$ (24%). At Harvard, the disagreement is larger, about 108 g C m $^{-2}$ y $^{-1}$ in the red oak-red maple forest and 282 g C m $^{-2}$ y $^{-1}$ in the hemlock stand.

The long-term trend of increasing NEP at Howland of 2.4 ± 2.1 g C m⁻² y⁻¹ is modest (values in this paragraph are mean \pm 95% confidence interval), about 1% per year, significant (P = 0.025), and requires explanation. Note that the present value is only about 25% (but within the uncertainties) of the non-significant trend reported previously for Howland (Keenan et al., 2013) using a much shorter data record. To put the magnitude of the Howland rate in context, Baldocchi et al. (2001) reported that an increase of one day in growing season length in a variety of forests was worth about 6 g C m⁻² y⁻¹.

Although many sites have published flux records in excess of 10 years, few if any exhibit a significant trend in the annual record. This is due to a combination of variability and the relatively short records, and of course the possibility of no trend existing. There is no significant trend in the 24-year record of NEP at the Harvard Forest (Finzi et al., 2020) or the 17-year record of a mixed deciduous/pine/transition forest at Camp Borden in Ontario, Canada (Froelich et al., 2015). Although trends in individual sites may lack statistical significance, considering a population of sites is also useful. Baldocchi (2020) found that the majority of 26 sites with >10-year records showed an increasing trend in NEE with an average rate of increase of $8.9 \pm 7.5 \text{ g C m}^{-2} \text{ y}^{-1}$.

At Howland, NEP is increasing not because of increased photosynthetic production (GPP is actually decreasing, -5.8 ± 4.2 g C m⁻² y⁻¹, P = 0.01), but because R_{eco} is decreasing with time more quickly (-8.2 ± 4.3 g C m⁻² y⁻¹, P < 0.001). This is at odds with the results in two other long-term studies. At the Harvard Forest oak-maple stand (Finzi et al., 2020) both GPP and R_{eco} are increasing (by 23 and 16 g C m⁻² y⁻¹) while at Camp Borden GPP is increasing and R_{eco} is decreasing (respectively 11.6 and -4.2 g C m⁻² y⁻¹).

What could be driving the different pattern at Howland and is it related to differences in forest type? Our results (Figure 10) show negative (although not always significant) trends in GPP every month across the April to October evergreen "active season". Consistently decreasing GPP argues against an exclusive influence of increasing CO₂ fertilization or season length. Age-related declines in tree and forest GPP are well known (Yoder et al., 1994) and often ascribed to reduced stomatal conductance. However, aging is not generally associated with steep declines in R_{eco}. Classically (e.g., Odum, 1969) it was believed that ecosystem respiration increased with age, rising to meet GPP and leading to forest C neutrality, but recent findings suggest otherwise.

Pregitzer and Euskirchen (2004) observed respiration to be highest in young, recently disturbed forests and argued against the classic model of respiration increasing with forest age. Curtis and Gough (2018) found no evidence for a steep decline in NEP during mid-succession in temperate deciduous (but not evergreen) forests and postulated that moderate disturbance might sustain higher than expected NEP in aging forests by introducing physical and biological complexity leading to the redistribution of growth-limiting resources and enhancing resource-use efficiency. The recent analysis of Xu et al. (2020) is perhaps most relevant. These authors looked specifically at resource use efficiency across deciduous and evergreen forests of different ages. They found that light and water resource use efficiencies (RUEs) declined with age in evergreen needleleaf forests but increased in deciduous forests. They found that the largest component of change in these RUEs was in maximum photosynthesis (A_{max}). Xu et al. (2020) further showed that derived A_{max} across age sequences for both evergreen and deciduous forest was strongly related to soil nitrogen concentration (N%) in the top 20 cm and that soil N% increased with age in deciduous forests and decreased with age in evergreen needleleaf forests. Mechanisms accounting for declining N% in evergreens but not deciduous forests would be lower quality (high C:N) litter, and reduced decomposition in cooler, shadier, evergreen forests. The connection to GPP and Reco is via foliar N, which is tightly correlated with soil N, and the strong relationship between N and light-saturated photosynthesis, particularly in temperate forests (Ollinger et al., 2002, 2008; Walker et al., 2014).

Instead, the small yet significant annual flux trends could result from interactions among the highly variable state factors that have not shown any long-term trends at Howland Forest over the sampling period. There is reason to believe that increasing temperatures at Howland Forest will increase annual GPP and ecosystem respiration. However, the effect on NEP might be offset by differential responses of spring and summer uptake versus temperature (e.g., Figure 11). The lack of significant trends in temperature and pre-

HOLLINGER ET AL. 14 of 21



cipitation over the sampling period have not resulted in a significant change in growing season, and only small, long-term trends in annual carbon exchange. Slight declines in annual GPP and ecosystem respiration are occurring despite modest increases in living biomass and LAI.

The improving air quality at the Howland Forest (Figure 3) may also contribute to some of the observed patterns. Excess nitrogen deposition may lead to reduced soil respiration (e.g., Janssens et al., 2010) and enhanced GPP (Fleischer et al., 2013), but it has also been specifically associated with enhanced foliage respiration in red spruce, a key component of the Howland Forest (McLaughlin & Kohut, 1992). A decline in N deposition and a regional recovery of red spruce growth has been observed with reduced N deposition (Kosiba et al., 2018), including at Howland (Teets, Fraver, Weiskittel, & Hollinger, 2018) and could potentially account for both decreasing GPP and $R_{\rm eco}$. In this case the change in N input may have accelerated the natural, age-related decline in evergreen resource use efficiency.

Higher levels of tropospheric ozone have deleterious effects on tree growth and often enhance aboveground respiration (see Grulke & Heath, 2020 for a comprehensive review). However, high ozone generally also depresses GPP, so the decrease in ozone might be expected to lead to a decrease in $R_{\rm eco}$ but an increase in GPP. It may be possible to better determine the relative role of ozone and N (or S) deposition at Howland based on their understood mode of action. Ozone, for example is a cumulative phytotoxin and may make its effects felt most late in the season.

5.3. Carbon Mass Balance Budget

A mass balance was derived from measurements and from calculation of additional component fluxes by differences, sums, or products of fluxes, as described in Table 2 and illustrated in Figure 12. The average of the NASA megaplot and the inventory plots was used for the estimated annual growth of live biomass. Total belowground carbon allocation (TBCA) was calculated from the difference between annual mean soil respiration and fine litterfall, which assumes that soil C stocks are at quasi steady state (Davidson et al., 2002). Total aboveground C allocation (TACA) was calculated from the difference between GPP and TBCA. The remaining formulas are presented in Table 2. The standard deviations of the annually measured components were calculated from their interannual variation. For the component fluxes we generated standard deviations of calculated flux components by randomly sampling 100,000 Monte Carlo estimates from a normal distribution.

The long-term mean annual growth of live biomass (161 ± 23 g C m⁻² yr⁻¹) accounts for about 80% (but see below) of the long-term mean annual NEP (211 ± 40 g C m⁻² yr⁻¹; Table 2). Based on previous lysimeter studies at the same site (Fernandez et al., 1995), leaching of DOC was estimated at only 3 ± 1 g C m⁻² yr⁻¹. Annual emissions of isoprene and other hydrocarbons were not measured but likely represent <4 g C m⁻² yr⁻¹ (Fuentes & Wang, 1999; Goldstein et al., 1998). By difference we estimate that there could be a sink of 48 ± 46 g C m⁻² yr⁻¹ in a combination of increasing soil organic matter and dead wood stocks. Given the large uncertainty of this estimate, we do not have confidence that the sink is significantly different from zero, nor do our data and mass balance calculations enable us to distinguish between soil and dead wood as the potential C sinks. Using radiocarbon, Gaudinski et al. (2000) estimated that the soil sink at the Harvard Forest of Massachusetts could be on the order of 20 ± 10 g C m⁻² yr⁻¹, which is within that range of our calculated budget for the Howland forest. In any case, the soil and dead wood sinks, if they are different from zero, are small relative to the measured NEP.

The measurements of biomass increment in the megaplot and inventory plots yielded estimates that accounted for 72% and 84% of the tower-based NEP measurements, respectively. These ratios are within the range of two synthesis studies comparing biomass increment to tower-based measurements of NEP. Biomass increment accounted for 94% \pm 37% of NEP across five North American forests (Curtis et al., 2002) and 59% \pm 17% across five European forests (Babst et al., 2014), with the assumption that belowground woody biomass accumulation represents 22% of the aboveground biomass growth in the latter study (Chojnacky et al., 2014).

Our carbon mass balance also provides insights into components of the carbon budget. For example, the mean annual soil respiration (816 \pm 108 g C m⁻² yr⁻¹) at the Howland Forest is about 73% of mean an-

HOLLINGER ET AL. 15 of 21



Table 2
Mass Balance Carbon Budget

Flux term	Abbreviation	Mean g C m ⁻² yr ⁻¹	Std. Dev. g C m ⁻² yr ⁻¹	Data source or calculation
Gross primary production	GPP	1325	84	Eddy covariance
Total ecosystem respiration	Reco	1114	96	Eddy covariance
Net ecosystem production	NEP	211	40	Eddy covariance
Biomass growth	$\Delta Biomass$	161	23	Biomass biometry
Soil respiration	R_soil	816	108	Chamber flux measurements
Fine litterfall	L_fine	167	23	Litterfall collectors
Aboveground net primary production	ANPP	328	33	$\Delta Biomass + L_fine$
Dissolved organic carbon export	DOC	3	1	Lysimeters (Fernandez et al., 1995)
Total belowground carbon allocation	TBCA	649	111	Rsoil - Lfine
Total aboveground carbon allocation	TACA	676	140	GPP - TBCA
Respiration from SOM decomposition	R_SOM	384	51	R_soil * 0.47; (Carbone et al., 2016)
Dead wood respiration	R_CWD	34	4	Necromass biometry & decomposition coefficients
Total heterotrophic respiration	R_hetero	418	51	R_SOM + R_CWD
Root (rhizosphere) respiration	R_root	432	57	R_soil * 0.53; (Carbone et al., 2016)
Leaf and stem respiration	R_leaf&stem	264	120	R_auto - R_root
Total autotrophic respiration	R_auto	696	109	R_eco - R_hetero
Root litter production	L_root	217	117	TBCA - R_root
Total net primary production	NPP	544	121	$\Delta Biomass + L_fine + L_root$
Dead wood litter production	L_CWD	84	27	TACA - ΔBiomass - R_leaf&stem - L_fine
Change in SOM and dead wood carbon	$\Delta SOM + CWD$	48	46	NEP - ΔBiomass - DOC

nual total ecosystem respiration (1114 \pm 80 g C m⁻² yr⁻¹; Table 2), which is in alignment with studies at the Harvard Forest (Finzi et al., 2020) and other temperate forests (Davidson et al., 2002). Mean annual allocation of C above ground (683 \pm 137 g C m⁻² yr⁻¹) is about equal to mean annual belowground C allocation (649 \pm 111 g C m⁻² yr⁻¹; Table 2). This estimate of belowground carbon allocation, based on the difference between annual soil respiration and annual litterfall (Davidson et al., 2002), when combined with partitioning of soil respiration into autotrophic and heterotrophic components (Carbone et al., 2016), allows us to calculate root litter production, also known as belowground net primary productivity (BNPP), as 217 ± 117 g C m⁻² yr⁻¹; Table 2). We estimate that BNPP is about 40% of total net primary productivity (NPP) of 544 ± 121 g C m⁻² yr⁻¹, which is the sum of BNPP, litterfall, and biomass increment. Finzi et al. (2020) used data from sequential root coring and minirhizotrons to estimate that BNPP is 332 ± 117 g C m⁻² yr⁻¹) at the Harvard Forest, which is 38%-47% of total NPP, although they note large uncertainties in those methods for measuring root production. Our mass balance yields similar estimates of the fraction of total NPP that is allocated belowground, using constraints from more feasibly measured C fluxes. These mass balance calculations assume that the soil and litter pools are at steady state, which may not be strictly true, but as already noted above, the calculated soil C sink is not significantly different from zero and in any case is small.

5.4. Long Term Measurements and Forests as Natural Carbon Solutions

In addition to climate-induced changes on forest carbon-cycle processes, such as the impact of drought, Anderegg et al. (2020) note that climate-induced changes in disturbance events such as fire, windthrow, or insect outbreaks may also be a risk to forest C permanence. The risk of disturbance discounts the value of carbon stored in a NCS. However, stand-replacing disturbances are relatively rare in the northeast U.S. (Anderegg et al., 2020; Pugh et al., 2019). Climate-induced changes in disturbance may represent a more serious threat to NCS permanence in other regions. While the Howland Forest has experienced wide var-

HOLLINGER ET AL. 16 of 21

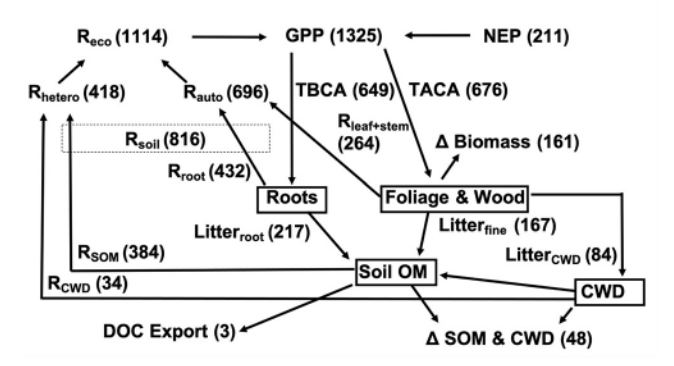


Figure 12. Summary of the Howland carbon cycle processes. Carbon stocks and fluxes across different ecosystem components are averaged over multi-decadal measurements of eddy covariance fluxes, soil chamber fluxes, and biometric inventories. All values are g C m^{-2} y^{-1} .

iations in climate, we know of no natural stand-replacing disturbances at the Howland Forest during the last century and have evidence of only some limited selective logging about 100 years ago.

Eddy covariance and associated data can have a key role in understanding the functioning of Natural Climate Solutions (Baldocchi & Penuelas, 2019; Hemes et al., 2021). This applies especially with assessing hard-to-observe carbon pools such as soils, important non-CO₂ greenhouse gas fluxes, and changes in ecosystem energy balance (Hemes et al., 2021). Based on our own experiences, however, we are more cautious about the use of eddy flux methods for commercial-scale accounting of forest C storage, especially in lieu of inventory data (e.g., Bautista et al., 2021; Marino et al., 2019). Marino et al. (2019) argued that a greater than 10-fold disparity between Howland eddy flux results and inventory data collected to register the Howland Forest as a Climate Action Reserve under the California Air Resources Board (CARB) should invalidate the approach of the registry. However, the difference exists because credit was given for initial standing live carbon stocks at Howland that greatly exceeded the

average standing live carbon stocks on similar lands within the region (Section 6.2.1, Compliance Offset Protocols U.S. Forest Projects, https://www.arb.ca.gov/regact/2010/capandtrade10/copusforest.pdf). This feature helps preserve land with the highest initial C stocks and does not invalidate inventory approaches. Inventories have other useful features including spatial averaging, ease of application, and a retained record of C changes. By combining inventory and flux data, we have demonstrated the relative permanence of a large standing stock of carbon and a fairly consistent net sink of carbon at the Howland Forest during the last three decades.

6. Conclusions

Over 25 years of measurement (including the warmest, wettest, and driest years in the last 125), the mature, unmanaged Howland forest has maintained an average annual carbon sink of just over 200 g m $^{-2}$ y $^{-1}$. These long-term measurements have allowed the detection of a small but significant trend of increasing NEP at Howland. Over 75% of the eddy flux measured carbon can be accounted for in biomass increments from inventories carried out within the tower footprint, although they did not confirm a trend of increasing carbon storage. Interannual variability in both flux and inventory data is such that the differences between the two are not significant. Seasonal variations in temperature can account for some of the large interannual variation in NEP that was observed (e.g., higher values in years with early springs) as has been observed previously at Howland and elsewhere.

The increase in NEP seems to be caused by statistically significant decreases in GPP and $R_{\rm eco}$ over time where the decline in $R_{\rm eco}$ has outpaced that in GPP. This apparent slowing of carbon cycling into and out of this system is difficult to explain based on variations in climate or increasing atmospheric CO_2 . However, these results support the idea that decreasing nitrogen use efficiency occurs in aging evergreen forests as N becomes less available (Xu et al., 2020). Decreased N deposition may have accelerated the trend of reduced N availability and account for some of the decline in GPP and $R_{\rm eco}$ and consequent increase in NEP.

Overall, in the Howland Forest we find surprising stability in annual carbon sequestration despite substantial demographic, climatic, and chemical changes. The age-related patterns of NEP and component C fluxes revealed by long-term research sites will help pave the way towards fully utilizing natural climate solutions.

Conflict of Interest

There are no conflicts of interest for any author.

HOLLINGER ET AL. 17 of 21



Data Availability Statement

All data used in this study (gap-filled flux data, soil respiration data, inventory measurements, LAI, phenology, litterfall, and other data), are available from the USDA Forest Service Research Data Archive (https://doi.org/10.2737/RDS-2021-0014). Additional Howland data are available from AmeriFlux (see https://ameriflux.lbl.gov/data/how-to-uploaddownload-data/). PhenoCam data are archived at the ORNL DAAC (https://daac.ornl.gov/cgi-bin/dsviewer.pl?ds_id=1689). Image in Figure 1 Copyright (c) Brian R. Hall licensed for use under a Creative Commons Attribution Non-Commercial No Derivatives License (CC BY-NC-ND). https://ark.digitalcommonwealth.org/ark:/50959/vh53xs848

Acknowledgments

The findings and conclusions in this publication are those of the author(s) and should not be construed to represent any official USDA or U.S. Government determination or policy. Funding for this AmeriFlux core site was provided by the U.S. Department of Energy's Office of Science. Additional support was provided by USDA NIFA award #2014-67003-22073, the USDA Forest Service Northern Research Station, and the Maine Agricultural and Forest Experiment Station. ADR acknowledges support for PhenoCam through NSF's Macrosystems Biology program (EF-1702697). The authors wish to acknowledge George Woodwell and Ivan Fernandez for their vision and actions for enabling long-term ecosystem science studies to be established at the Howland Forest site.

References

- Anderegg, W. R., Trugman, A. T., Badgley, G., Anderson, C. M., Bartuska, A., Ciais, P., et al. (2020). Climate-driven risks to the climate mitigation potential of forests. Science, 368(6497). https://doi.org/10.1126/science.aaz7005
- Babst, F., Alexander, M. R., Szejner, P., Bouriaud, O., Klesse, S., Roden, J., et al. (2014). A tree-ring perspective on the terrestrial carbon cycle. Oecologia, 176(2), 307–322. https://doi.org/10.1007/s00442-014-3031-6
- Baldocchi, D., Chu, H., & Reichstein, M. (2018). Inter-annual variability of net and gross ecosystem carbon fluxes: A review. Agricultural and Forest Meteorology, 249, 520–533. https://doi.org/10.1016/j.agrformet.2017.05.015
- Baldocchi, D., Falge, E., Gu, L., Olson, R., Hollinger, D., Running, S., et al. (2001). FLUXNET: A new tool to study the temporal and spatial variability of ecosystem-scale carbon dioxide, water vapor, and energy flux densities. *Bulletin of the American Meteorological Society*, 82(11), 2415–2434. https://doi.org/10.1175/1520-0477(2001)082<2415:FANTTS>2.3.CO;2
- Baldocchi, D., & Penuelas, J. (2019). The physics and ecology of mining carbon dioxide from the atmosphere by ecosystems. Global Change Biology, 25(4), 1191–1197. https://doi.org/10.1111/gcb.14559
- Baldocchi, D. D. (2020). How eddy covariance flux measurements have contributed to our understanding of Global Change Biology. Global Change Biology, 26(1), 242–260. https://doi.org/10.1111/gcb.14807
- Bautista, N., Marino, B. D., & Munger, J. W. (2021). Science to commerce: A commercial-scale protocol for carbon trading applied to a 28-year record of forest carbon monitoring at the Harvard Forest. Land, 10(2), 163. https://doi.org/10.3390/land10020163
- Bowling, D. R., Logan, B. A., Hufkens, K., Aubrecht, D. M., Richardson, A. D., Burns, S. P., et al. (2018). Limitations to winter and spring photosynthesis of a Rocky Mountain subalpine forest. *Agricultural and Forest Meteorology*, 252, 241–255. https://doi.org/10.1016/j.agrformet.2018.01.025
- Carbone, M. S., Richardson, A. D., Chen, M., Davidson, E. A., Hughes, H., Savage, K. E., & Hollinger, D. Y. (2016). Constrained partitioning of autotrophic and heterotrophic respiration reduces model uncertainties of forest ecosystem carbon fluxes but not stocks. *Journal of Geophysical Research: Biogeosciences*, 121(9), 2476–2492. https://doi.org/10.1002/2016jg003386
- Carrara, A., Kowalski, A.S., Neirynck, J., Janssens, I.A., Yuste, J.C., & Ceulemans, R. (2003). Net ecosystem CO₂ exchange of mixed forest in Belgium over 5 years. *Agricultural and Forest Meteorology*, 119(3–4), 209–227. https://doi.org/10.1016/S0168-1923(03)00120-5
- Chen, J. M., Govind, A., Sonnentag, O., Zhang, Y., Barr, A., & Amiro, B. (2006). Leaf area index measurements at Fluxnet-Canada forest sites. *Agricultural and Forest Meteorology*, 140(1), 257–268. https://doi.org/10.1016/j.agrformet.2006.08.005
- Chojnacky, D. C., Heath, L. S., & Jenkins, J. C. (2014). Updated generalized biomass equations for North American tree species. *Forestry*, 87(1), 129–151. https://doi.org/10.1093/forestry/cpt053
- Curtis, P. S., & Gough, C. M. (2018). Forest aging, disturbance and the carbon cycle. New Phytologist, 219(4), 1188–1193. https://doi.org/10.1111/nph.15227
- Curtis, P. S., Hanson, P. J., Bolstad, P., Barford, C., Randolph, J.C., Schmid, H., & Wilson, K. B. (2002). Biometric and eddy-covariance based estimates of annual carbon storage in five eastern North American deciduous forests. Agricultural and Forest Meteorology, 113(1-4), 3-19. https://doi.org/10.1016/S0168-1923(02)00099-0
- Daly, C., Halbleib, M., Smith, J. I., Gibson, W. P., Doggett, M. K., Taylor, G. H., et al. (2008). Physiographically sensitive mapping of climatological temperature and precipitation across the conterminous United States. *International Journal of Climatology*, 28(15), 2031–2064. https://doi.org/10.1002/joc.1688
- Davidson, E. A., Savage, K., Bolstad, P., Clark, D. A., Curtis, P. S., Ellsworth, D. S., et al. (2002). Belowground carbon allocation in forests estimated from litterfall and IRGA-based soil respiration measurements. *Agricultural and Forest Meteorology*, 113(1), 39–51. https://doi.org/10.1016/s0168-1923(02)00101-6
- Day, M. E. (2000). Influence of temperature and leaf-to-air vapor pressure deficit on net photosynthesis and stomatal conductance in red spruce (Picea rubens). Tree Physiology, 20(1), 57–63. https://doi.org/10.1093/treephys/20.1.57
- Fargione, J. E., Bassett, S., Boucher, T., Bridgham, S. D., Conant, R. T., Cook-Patton, S. C., et al. (2018). Natural climate solutions for the United States. Science Advances, 4(11), eaat1869. https://doi.org/10.1126/sciadv.aat1869
- Felzer, B. S., Cronin, T., Reilly, J. M., Melillo, J. M., & Wang, X. (2007). Impacts of ozone on trees and crops. Comptes Rendus Geoscience, 339(11), 784–798. https://doi.org/10.1016/j.crte.2007.08.008
- Fernandez, I. J., Lawrence, G. B., Son, Y., & Howland (1995). Soil-solution chemistry in a low-elevation spruce-fir ecosystem. Water, Air, and Soil Pollution, 84(1), 129–145. https://doi.org/10.1007/BF00479593
- Fernandez, I. J., Rustad, L. E., & Lawrence, G. B. (1993). Estimating total soil mass, nutrient content, and trace metals in soils under a low elevation spruce-fir forest. Canadian Journal of Soil Science, 73(3), 317–328. https://doi.org/10.4141/cjss93-034
- Fien, E. K. P., Fraver, S., Teets, A., Weiskittel, A. R., & Hollinger, D. Y. (2019). Drivers of individual tree growth and mortality in an une-ven-aged, mixed-species conifer forest. Forest Ecology and Management, 449, 117446. https://doi.org/10.1016/j.foreco.2019.06.043
- Finkelstein, P. L., & Sims, P. F. (2001). Sampling error in eddy correlation flux measurements. *Journal of Geophysical Research*, 106(D4), 3503–3509. https://doi.org/10.1029/2000id900731
- Finzi, A. C., Giasson, M.-A., Barker Plotkin, A. A., Aber, J. D., Boose, E. R., Davidson, E. A., et al. (2020). Carbon budget of the Harvard Forest Long-Term Ecological Research site: Pattern, process, and response to global change. *Ecological Monographs*, 90(4), e01423. https://doi.org/10.1002/ecm.1423
- Fleischer, K., Rebel, K. T., Van Der Molen, M. K., Erisman, J. W., Wassen, M. J., Van Loon, E. E., et al. (2013). The contribution of nitrogen deposition to the photosynthetic capacity of forests. *Global Biogeochemical Cycles*, 27(1), 187–199. https://doi.org/10.1002/gbc.20026

HOLLINGER ET AL. 18 of 21



- Froelich, N., Croft, H., Chen, J. M., Gonsamo, A., & Staebler, R. M. (2015). Trends of carbon fluxes and climate over a mixed temperate-boreal transition forest in southern Ontario, Canada. Agricultural and Forest Meteorology, 211–212, 72–84. https://doi.org/10.1016/j.agrformet.2015.05.009
- Fuentes, J. D., & Wang, D. (1999). On the seasonality of isoprene emissions from a mixed temperate forest. *Ecological Applications*, 9(4), 1118–1131. https://doi.org/10.1890/1051-0761(1999)009[1118:otsoie]2.0.co:2
- Gaudinski, J. B., Trumbore, S. E., Davidson, E. A., & Zheng, S. (2000). Soil carbon cycling in a temperate forest: Radiocarbon-based estimates of residence times, sequestration rates and partitioning of fluxes. Biogeochemistry, 51(1), 33–69. https://doi.org/10.1023/A:1006301010014
- Goldstein, A. H., Goulden, M. L., Munger, J. W., Wofsy, S. C., & Geron, C. D. (1998). Seasonal course of isoprene emissions from a midlatitude deciduous forest. *Journal of Geophysical Research*, 103(D23), 31045–31056. https://doi.org/10.1029/98jd02708
- Gosz, J. R., Holmes, R. T., Likens, G. E., & Bormann, F. H. (1978). The flow of energy in a forest ecosystem. Scientific American, 238(3), 92–102. https://doi.org/10.1038/scientificamerican0378-92
- Griscom, B. W., Adams, J., Ellis, P. W., Houghton, R. A., Lomax, G., Miteva, D. A., et al. (2017). Natural climate solutions. Proceedings of the National Academy of Sciences, 114(44), 11645–11650. https://doi.org/10.1073/pnas.1710465114
- Grulke, N. E., & Heath, R. L. (2020). Ozone effects on plants in natural ecosystems. Plant Biology, 22(S1), 12–37. https://doi.org/10.1111/plb.12971
- Grünwald, T., & Bernhofer, C. (2007). A decade of carbon, water and energy flux measurements of an old spruce forest at the Anchor Station Tharandt. Tellus B: Chemical and Physical Meteorology, 59(3), 387–396. https://doi.org/10.3402/tellusb.v59i3.17000
- Harmon, M. E., Woodall, C. W., Fasth, B., & Sexton, J. (2008). Woody detritus density and density reduction factors for tree species in the United States: A synthesis. (Gen. Tech. Rep. NRS-29) (Vol. 84, p. 29). Newtown Square, PA: US Department of Agriculture, Forest Service, Northern Research Station. https://doi.org/10.2737/NRS-GTR-29
- Hemes, K. S., Runkle, B. R., Novick, K. A., Baldocchi, D. D., & Field, C. B. (2021). An ecosystem-scale flux measurement strategy to assess natural climate solutions. Environmental Science & Technology, 55(6), 3494–3504. https://doi.org/10.1021/acs.est.0c06421
- Hollinger, D. Y., Aber, J., Dail, B., Davidson, E. A., Goltz, S. M., Hughes, H., et al. (2004). Spatial and temporal variability in forest-atmosphere CO₂ exchange. Global Change Biology, 10(10), 1689–1706. https://doi.org/10.1111/j.1365-2486.2004.00847.x
- Hollinger, D. Y., Goltz, S. M., Davidson, E. A., Lee, J. T., Tu, K., & Valentine, H. T. (1999). Seasonal patterns and environmental control of carbon dioxide and water vapour exchange in an Ecotonal Boreal Forest. Global Change Biology, 5(8), 891–902. https://doi.org/10.1046/j.1365-2486.1999.00281.x
- Holmes, R. L. (1983). Computer-assisted quality control in tree-ring dating and measurements. Tree-Ring Bulletin, 44, 69–75. Retrieved from http://hdl.handle.net/10150/261223
- Hoover, C. M., Leak, W. B., & Keel, B. G. (2012). Benchmark carbon stocks from old-growth forests in northern New England, USA. Forest Ecology and Management, 266, 108–114. https://doi.org/10.1016/j.foreco.2011.11.010
- Janssens, I. A., Dieleman, W., Luyssaert, S., Subke, J. A., Reichstein, M., Ceulemans, R., et al. (2010). Reduction of forest soil respiration in response to nitrogen deposition. *Nature Geoscience*, 3(5), 315–322. https://doi.org/10.1038/ngeo844
- Keenan, T. F., Hollinger, D. Y., Bohrer, G., Dragoni, D., Munger, J. W., Schmid, H. P., & Richardson, A. D. (2013). Increase in forest water-use efficiency as atmospheric carbon dioxide concentrations rise. *Nature*, 499(7458), 324–327. https://doi.org/10.1038/nature12291
- Kljun, N., Calanca, P., Rotach, M. W., & Schmid, H. P. (2015). A simple two-dimensional parameterisation for Flux Footprint Prediction (FFP). Geoscientific Model Development, 8(11), 3695–3713. https://doi.org/10.5194/gmd-8-3695-2015
- Kosiba, A. M., Schaberg, P. G., Rayback, S. A., & Hawley, G. J. (2018). The surprising recovery of red spruce growth shows links to decreased acid deposition and elevated temperature. The Science of the Total Environment, 637–638, 1480–1491. https://doi.org/10.1016/j.scitotenv.2018.05.010
- Kunkel, K. E., Stevens, L. E., Stevens, S. E., Sun, L., Janssen, E., Wuebbles, D., et al. (2013). Regional climate trends and scenarios for the US national climate assessment. Part 1. Climate of the northeast US. (NOAA technical report NESDIS 142-1). (p. 87). Washington, DC: National Oceanic and atmospheric administration, National Environmental Satellite, Data, and Information Service. Retrieved from https://scenarios.globalchange.gov/sites/default/files/NOAA_NESDIS_Tech_Report_142-1-Climate_of_the_Northeast_U.S_1.pdf
- Lamlom, S. H., & Savidge, R. A. (2003). A reassessment of carbon content in wood: Variation within and between 41 North American species. Biomass and Bioenergy, 25(4), 381–388. https://doi.org/10.1016/S0961-9534(03)00033-3
- Lee, X., Goulden, M. L., Hollinger, D. Y., Barr, A., Black, T. A., Bohrer, G., et al. (2011). Observed increase in local cooling effect of deforest-ation at higher latitudes. Nature, 479(7373), 384–387. https://doi.org/10.1038/nature10588
- Levine, E. R., Knox, R. G., & Lawrence, W. T. (1994). Relationships between soil properties and vegetation at the Northern Experimental Forest, Howland, Maine. Remote Sensing of Environment, 47(2), 231–241. https://doi.org/10.1016/0034-4257(94)90158-9
- Liu, J., Wennberg, P. O., Parazoo, N. C., Yin, Y., & Frankenberg, C. (2020). Observational constraints on the response of high-latitude northern forests to warming. AGU Advances, 1(4), e2020AV000228. https://doi.org/10.1029/2020AV000228
- Marino, B. D., Mincheva, M., & Doucett, A. (2019). California air resources board forest carbon protocol invalidates offsets. PeerJ, 7, e7606. https://doi.org/10.7717/peerj.7606
- McLaughlin, S. B., & Kohut, R. J. (1992). The effects of atmospheric deposition and ozone on carbon allocation and associated physiological processes in red spruce. In Eagar, C., & Adams, M. B. (Eds.), Ecology and decline of red spruce in the eastern United States (pp. 338–382). New York, NY: Springer New York. https://doi.org/10.1007/978-1-4612-2906-3_9
- McMillen, R. T. (1988). An eddy correlation technique with extended applicability to non-simple terrain. *Boundary-Layer Meteorology*, 43(3), 231–245. https://doi.org/10.1007/BF00128405
- Musselman, R. C., Lefohn, A. S., Massman, W. J., & Heath, R. L. (2006). A critical review and analysis of the use of exposure- and flux-based ozone indices for predicting vegetation effects. Atmospheric Environment, 40(10), 1869–1888. https://doi.org/10.1016/j. atmosenv.2005.10.064
- NOAA. (2021). NOAA National Centers for Environmental Information, climate at a glance: Regional time series. published May 2021, retrieved on May 19, 2021 from https://www.ncdc.noaa.gov/cag/
- Odum, E. P. (1969). The strategy of ecosystem development. Science, 164, 262-270. https://doi.org/10.1126/science.164.3877.262
- Ollinger, S. V., Richardson, A. D., Martin, M. E., Hollinger, D. Y., Frolking, S. E., Reich, P. B., et al. (2008). Canopy nitrogen, carbon assimilation, and albedo in temperate and boreal forests: Functional relations and potential climate feedbacks. *Proceedings of the National Academy of Sciences*, 105(49), 19336–19341. https://doi.org/10.1073/pnas.0810021105
- Ollinger, S. V., Smith, M. L., Martin, M. E., Hallett, R. A., Goodale, C. L., & Aber, J. D. (2002). Regional variation in foliar chemistry and N cycling among forests of diverse history and composition. *Ecology*, 83(2), 339–355. https://doi.org/10.1890/0012-9658(2002)083[033 9:rvifca]2.0.co;2

HOLLINGER ET AL. 19 of 21



- Pan, Y., Birdsey, R. A., Fang, J., Houghton, R., Kauppi, P. E., Kurz, W. A., et al. (2011). A large and persistent carbon sink in the world's forests. Science, 333(6045), 988–993. https://doi.org/10.1126/science.1201609
- Pregitzer, K. S., & Euskirchen, E. S. (2004). Carbon cycling and storage in world forests: Biome patterns related to forest age. Global Change Biology, 10(12), 2052–2077. https://doi.org/10.1111/j.1365-2486.2004.00866.x
- Pugh, T. A., Arneth, A., Kautz, M., Poulter, B., & Smith, B. (2019). Important role of forest disturbances in the global biomass turnover and carbon sinks. Nature Geoscience, 12(9), 730–735. https://doi.org/10.1038/s41561-019-0427-2
- Puhlick, J. J., Weiskittel, A. R., Fernandez, I. J., Fraver, S., Kenefic, L. S., Seymour, R. S., et al. (2016). Long-term influence of alternative forest management treatments on total ecosystem and wood product carbon storage. Canadian Journal of Forest Research, 46(11), 1404–1412. https://doi.org/10.1139/cjfr-2016-0193
- Ranson, K. J., Sun, G., Knox, R. G., Levine, E. R., Weishampel, J. F., & Fifer, S. T. (2001). Northern forest ecosystem dynamics using coupled models and remote sensing. Remote Sensing of Environment, 75(2), 291–302. https://doi.org/10.1016/S0034-4257(00)00174-7
- Ricciuto, D.M., Butler, M.P., Davis, K.J., Cook, B.D., Bakwin, P.S., Andrews, A., & Teclaw, R.M. (2008). Causes of interannual variability in ecosystem-atmosphere CO₂ exchange in a northern Wisconsin forest using a Bayesian model calibration. Agricultural and Forest Meteorology, 148(2), 309-327. https://doi.org/10.1016/j.agrformet.2007.08.007
- Richardson, A. D. (2019). Tracking seasonal rhythms of plants in diverse ecosystems with digital camera imagery. New Phytologist, 222(4), 1742–1750. https://doi.org/10.1111/nph.15591
- Richardson, A. D., Dail, D. B., & Hollinger, D. Y. (2011). Leaf area index uncertainty estimates for model-data fusion applications. Agricultural and Forest Meteorology, 151(9), 1287–1292. https://doi.org/10.1016/j.agrformet.2011.05.009
- Richardson, A. D., & Hollinger, D. Y. (2007). A method to estimate the additional uncertainty in gap-filled NEE resulting from long gaps in the CO₂ flux record. Agricultural and Forest Meteorology, 147(3), 199–208. https://doi.org/10.1016/j.agrformet.2007.06.004
- Richardson, A. D., Hollinger, D. Y., Dail, D. B., Lee, J. T., Munger, J. W., & O'keefe, J. (2009). Influence of spring phenology on seasonal and annual carbon balance in two contrasting New England forests. *Tree Physiology*, 29(3), 321–331. https://doi.org/10.1093/treephys/ tpn040
- Richardson, A. D., Hollinger, D. Y., Shoemaker, J. K., Hughes, H., Savage, K., & Davidson, E. A. (2019). Six years of ecosystem-atmosphere greenhouse gas fluxes measured in a sub-boreal forest. *Scientific Data*, 6(1), 117. https://doi.org/10.1038/s41597-019-0119-1
- Richardson, A. D., Hufkens, K., Milliman, T., Aubrecht, D. M., Chen, M., Gray, J. M., et al. (2018). Tracking vegetation phenology across diverse North American biomes using PhenoCam imagery. Scientific Data, 5(1), 180028. https://doi.org/10.1038/sdata.2018.28
- Russell, M. B., Woodall, C. W., Fraver, S., D'Amato, A. W., Domke, G. M., & Skog, K. E. (2014). Residence times and decay rates of downed woody debris biomass/carbon in eastern US forests. Ecosystems, 17(5), 765–777. https://doi.org/10.1007/s10021-014-9757-5
- Savage, K. E., & Davidson, E. A. (2001). Interannual variation of soil respiration in two New England forests. *Global Biogeochemical Cycles*, 15(2), 337–350. https://doi.org/10.1029/1999GB001248
- Savage, K. E., & Davidson, E. A. (2003). A comparison of manual and automated systems for soil CO₂ flux measurements: Trade-offs between spatial and temporal resolution. *Journal of Experimental Botany*, 54(384), 891–899. https://doi.org/10.1093/jxb/erg121
- Schmieden, U., & Wild, A. (1995). The contribution of ozone to forest decline. Physiologia Plantarum, 94(2), 371-378. https://doi.org/10.1034/i.1399-3054.1995.940227.x
- Seyednasrollah, B., Bowling, D. R., Cheng, R., Logan, B. A., Magney, T. S., Frankenberg, C., et al. (2021). Seasonal variation in the canopy color of temperate evergreen conifer forests. New Phytologist, 229, 2586–2600. https://doi.org/10.1111/nph.17046
- Seyednasrollah, B., Young, A. M., Hufkens, K., Milliman, T., Friedl, M. A., Frolking, S., & Richardson, A. D. (2019). Tracking vegetation phenology across diverse biomes using Version 2.0 of the PhenoCam Dataset. *Scientific Data*, 6(1), 222. https://doi.org/10.1038/s41597-019-0229-9
- Shoemaker, J. K., Keenan, T. F., Hollinger, D. Y., & Richardson, A. D. (2014). Forest ecosystem changes from annual methane source to sink depending on late summer water balance. Geophysical Research Letters, 41(2), 673–679. https://doi.org/10.1002/2013GL058691
- Sun, G., Ranson, K. J., Guo, Z., Zhang, Z., Montesano, P., & Kimes, D. (2011). Forest biomass mapping from LIDAR and radar synergies. Remote Sensing of Environment, 115(11), 2906–2916. https://doi.org/10.1016/j.rse.2011.03.021
- Tanja, S., Berninger, F., Vesala, T., Markkanen, T., Hari, P., Mäkelä, A., et al. (2003). Air temperature triggers the recovery of evergreen boreal forest photosynthesis in spring. Global Change Biology, 9(10), 1410–1426. https://doi.org/10.1046/j.1365-2486.2003.00597.x
- Teets, A., Fraver, S., Hollinger, D. Y., Weiskittel, A. R., Seymour, R. S., & Richardson, A. D. (2018). Linking annual tree growth with eddy-flux measures of net ecosystem productivity across twenty years of observation in a mixed conifer forest. Agricultural and Forest Meteorology, 249, 479–487. https://doi.org/10.1016/j.agrformet.2017.08.007
- Teets, A., Fraver, S., Weiskittel, A. R., & Hollinger, D. Y. (2018). Quantifying climate–growth relationships at the stand level in a mature mixed-species conifer forest. Global Change Biology, 24(8), 3587–3602. https://doi.org/10.1111/gcb.14120
- Vann, D. R., Johnson, A. H., & Casper, B. B. (1994). Effect of elevated temperatures on carbon dioxide exchange in Picea rubens. Tree Physiology, 14(12), 1339–1349. https://doi.org/10.1093/treephys/14.12.1339
- Van Wagner, C. E. (1968). The line intersect method in forest fuel sampling. Forest Science, 14(1), 20–26. https://doi.org/10.1093/forestscience/14.1.2010.1093/forestscience/14.4.455
- Walker, A. P., Beckerman, A. P., Gu, L., Kattge, J., Cernusak, L. A., Domingues, T. F., et al. (2014). The relationship of leaf photosynthetic traits-V_{cmax} and J_{max}-to leaf nitrogen, leaf phosphorus, and specific leaf area: A meta-analysis and modeling study. Ecology and evolution, 4(16), 3218–3235. https://doi.org/10.1002/ece3.1173
- Weishampel, J. F., Sung, G., Ransom, K. J., LeJeune, K. D., & Shugart, H. H. (1994). Forest textural properties from simulated microwave backscatter: The influence of spatial resolution. Remote Sensing of Environment, 47(2), 120–131. https://doi.org/10.1016/0034-4257(94)90149-x
- Whittaker, R. H., Bormann, F. H., Likens, G. E., & Siccama, T. G. (1974). The Hubbard Brook ecosystem study: Forest biomass and production. Ecological Monographs, 44(2), 233–254. https://doi.org/10.2307/1942313
- Wutzler, T., Lucas-Moffat, A., Migliavacca, M., Knauer, J., Sickel, K., Šigut, L., et al. (2018). Basic and extensible post-processing of eddy covariance flux data with REddyProc. Biogeosciences, 15(16), 5015–5030. https://doi.org/10.5194/bg-15-5015-2018
- Xu, H., Xiao, J., Zhang, Z., Ollinger, S. V., Hollinger, D. Y., Pan, Y., & Wan, J. (2020). Canopy photosynthetic capacity drives contrasting age dynamics of resource use efficiencies between mature temperate evergreen and deciduous forests. Global Change Biology, 26(11), 6156–6167. https://doi.org/10.1111/gcb.15312
- Yoder, B. J., Ryan, M. G., Waring, R. H., Schoettle, A. W., & Kaufmann, M. R. (1994). Evidence of reduced photosynthetic rates in old trees. Forest Science, 40(3), 513–527. https://doi.org/10.1093/forestscience/40.3.51310.25291/vr/1994-1-vr-513
- Young, H. E., Ribe, J. H., & Wainwright, K. (1980). Weight tables for tree and shrub species in Maine (Vol. 230). University of Maine, Life Sciences and Agriculture Experiment Station. Retrieved from https://digitalcommons.library.umaine.edu/cgi/viewcontent.cgi?article=1019&context=aes_miscreports

HOLLINGER ET AL. 20 of 21



References From the Supporting Information

- Brown, J. K. (1974). Handbook for inventorying downed woody material. (Gen. Tech. Rep. INT- 24) (p. 16). Ogden, UT: US Department of Agriculture, Forest Service, Intermountain Forest and Range Experiment Station. Retrieved from https://www.fs.usda.gov/treesearch/pubs/28647
- Fraver, S., Ducey, M. J., Woodall, C. W., D'Amato, A. W., Milo, A. M., & Palik, B. J. (2018). Influence of transect length and downed woody debris abundance on precision of the line-intersect sampling method. Forest Ecosystems, 5(1), 39. https://doi.org/10.1186/s40663-018-0156-9
- Fraver, S., Milo, A. M., Bradford, J. B., D'Amato, A. W., Kenefic, L., Palik, B. J., et al. (2013). Woody debris volume depletion through decay: Implications for biomass and carbon accounting. *Ecosystems*, 16(7), 1262–1272. https://doi.org/10.1007/s10021-013-9682-z
- Harmon, M. E., Woodall, C. W., Fasth, B., & Sexton, J. (2008). Woody detritus density and density reduction factors for tree species in the United States: A synthesis. (Gen. Tech. Rep. NRS-29) (Vol. 84, p. 29). Newtown Square, PA: US Department of Agriculture, Forest Service, Northern Research Station. https://doi.org/10.2737/NRS-GTR-29
- Sollins, P. (1982). Input and decay of coarse woody debris in coniferous stands in western Oregon and Washington. Canadian Journal of Forest Research, 12(1), 18–28. https://doi.org/10.1139/x82-003
- Van Wagner, C. E. (1968). The line intersect method in forest fuel sampling. Forest Science, 14(1), 20–26. https://doi.org/10.1093/forestscience/14.1.2010.1093/forestscience/14.4.455
- Young, H. E., Ribe, J. H., & Wainwright, K. (1980). Weight tables for tree and shrub species in Maine (Vol. 230). University of Maine, Life Sciences and Agriculture Experiment Station. Retrieved from https://digitalcommons.library.umaine.edu/cgi/viewcontent.cgi?article=1019&context=aes_miscreports

HOLLINGER ET AL. 21 of 21